Comparative Transcriptome Analysis of Three Oil Palm Fruit and Seed Tissues That Differ in Oil Content and Fatty Acid Composition

Stéphane Dussert, Chloe Guerin, Mariette Andersson, Thierry Joet, Timothy J. Tranbarger, Maxime Pizot, Gautier Sarah, Alphonse Omore, Tristan Durand-Gasselin, Fabienne Morcillo

Comparative Transcriptome Analysis of Three Oil Palm Fruit and Seed Tissues That Differ in Oil Content and Fatty Acid Composition[1][C][W][OA]

Stéphane Dussert*, Chloé Guerin, Mariette Andersson, Thierry Joët, Timothy J. Tranbarger, Maxime Pizot[2], Gautier Sarah, Alphonse Omore, Tristan Durand-Gasselin, and Fabienne Morcillo

Institut de Recherche pour le Développement, Unité Mixte de Recherche Diversité, Adaptation et Développement des Plantes, BP 64501, 34394 Montpellier, France (S.D., T.J., T.J.T., M.P.); PalmElit, F-34980 Montferrier-sur-Lez, France (C.G., T.D.-G.); Department of Plant Breeding, Swedish University of Agricultural Sciences, SE–23053 Alnarp, Sweden (M.A.); Institut National de la Recherche Agronomique, Unité Mixte de Recherche Amélioration Génétique et Adaptation des Plantes Méditerranéennes et Tropicales, F–34398 Montpellier, France (G.S.); Institut National des Recherches Agricoles du Bénin, Centre de Recherches Agricoles Plantes Pérennes, Pobé, Benin (A.O.); and Centre de Coopération Internationale en Recherche Agronomique pour le Développement, Unité Mixte de Recherche Diversité, Adaptation et Développement des Plantes, F–34398 Montpellier, France (F.M.)

ORCID IDs: 0000-0002-9769-5288 (M.A.); 0000-0001-6278-8321 (T.J.T.).

Oil palm (*Elaeis guineensis*) produces two oils of major economic importance, commonly referred to as palm oil and palm kernel oil, extracted from the mesocarp and the endosperm, respectively. While lauric acid predominates in endosperm oil, the major fatty acids (FAs) of mesocarp oil are palmitic and oleic acids. The oil palm embryo also stores oil, which contains a significant proportion of linoleic acid. In addition, the three tissues display high variation for oil content at maturity. To gain insight into the mechanisms that govern such differences in oil content and FA composition, tissue transcriptome and lipid composition were compared during development. The contribution of the cytosolic and plastidial glycolytic routes differed markedly between the mesocarp and seed tissues, but transcriptional patterns of genes involved in the conversion of sucrose to pyruvate were not related to variations for oil content. Accumulation of lauric acid relied on the dramatic up-regulation of a specialized acyl-acyl carrier protein thioesterase paralog and the concerted recruitment of specific isoforms of triacylglycerol assembly enzymes. Three paralogs of the WRINKLED1 (WRI1) transcription factor were identified, of which *EgWRI1-1* and *EgWRI1-2* were massively transcribed during oil deposition in the mesocarp and the endosperm, respectively. None of the three *WRI1* paralogs were detected in the embryo. The transcription level of FA synthesis genes correlated with the amount of *WRI1* transcripts and oil content. Changes in triacylglycerol content and FA composition of *Nicotiana benthamiana* leaves infiltrated with various combinations of *WRI1* and *FatB* paralogs from oil palm validated functions inferred from transcriptome analysis.

Vegetable oils are predominantly composed of triacylglycerols (TAGs), which consist of glycerol esterified with three fatty acids (FAs). The diverse uses of vegetable oils primarily depend on the FA composition of TAG. For instance, a high proportion of lauric acid (12:0) is demanded for soap production, whereas oils rich in oleic acid (18:1) are recommended for cooking (Dyer et al., 2008). Plants store oil in various fruit and seed tissues, such as the mesocarp, the perisperm, the endosperm, and the embryo, but can also accumulate oil in leaves and stems (Lersten et al., 2006; Durrett et al., 2008). Furthermore, TAG accumulation and FA composition vary considerably among plants and tissues. Considering the constant increase in global demand for vegetable oils used both for food and industrial purposes, the identification of factors regulating these quantitative and qualitative variations is a critical issue, which is the focus of a growing number of studies (for review, see Baud and Lepiniec, 2010; Chapman and Ohlrogge, 2012).

The oil palm (*Elaeis guineensis*) fruit is a drupe with a thick, fleshy mesocarp surrounding a hardened endocarp that contains a large seed made of a copious endosperm and a tiny embryo. The mesocarp and the

[1] This work was supported by PalmElit, Institut de Recherche pour le Développement, Centre de Coopération Internationale en Recherche Agronomique pour le Développement, the SouthGreen Bioinformatics Platform (http://southgreen.cirad.fr/), and the high performance cluster of the Unité Mixte de Recherche Amélioration Génétique et Adaptation des Plantes Méditerranéennes et Tropicales, Centre de Coopération Internationale en Recherche Agronomique.

[2] Present address: VILMORIN SA, Centre de Recherche la Costière, Pazac, 30210 Lédenon, France.

* Corresponding author; e-mail stephane.dussert@ird.fr.

The author responsible for distribution of materials integral to the findings presented in this article in accordance with the policy described in the Instructions for Authors (www.plantphysiol.org) is: Stéphane Dussert (stephane.dussert@ird.fr).

[C] Some figures in this article are displayed in color online but in black and white in the print edition.

[W] The online version of this article contains Web-only data.

[OA] Open Access articles can be viewed online without a subscription.

www.plantphysiol.org/cgi/doi/10.1104/pp.113.220525

endosperm of oil palm are well known for their exceptionally high oil content (approximately 85% and 50% dry mass, respectively), making this crop unique in that it produces two oils of major economic importance, commonly referred to as palm oil and palm kernel oil. The FA composition of palm oil and palm kernel oil differs considerably. While medium-chain FAs (MCFAs; C8–C14) predominate in the endosperm, the major FAs of mesocarp oil are palmitic acid (16:0) and 18:1. Given that oils rich in MCFA and palmitate are the preferred materials in various industries (Durrett et al., 2008), and that the intake of fats rich in palmitic acid (16:0) as a potential cause of cardiovascular diseases is still a matter of debate (Willett, 2012), a better understanding of the molecular determinants for high levels of saturated FA is of key importance.

In plants, de novo FA synthesis occurs in the plastid and consists of sequential reactions of condensation, reduction, and dehydration that add two-carbon units to the elongating acyl chain, which remains conjugated to acyl carrier protein (ACP) during this cyclic process. The transfer of nascent FA to the endoplasmic reticulum (ER) for TAG assembly requires the hydrolysis of acyl-ACP to release free FA. This reaction is catalyzed by acyl-ACP thioesterases. Plant acyl-ACP thioesterases separate into two classes, termed FatA and FatB (Jones et al., 1995). It is typically accepted that enzymes of the FatA class preferentially hydrolyze 18:1-ACP whereas saturated acyl-ACP would be the preferential substrate of FatB thioesterases. Transcription of *FatB* is usually low in comparison with *FatA* in the developing seeds of Arabidopsis (*Arabidopsis thaliana*) and temperate oil crops whose seeds accumulate TAG with low saturated FA levels (Dörmann et al., 2000; Troncoso-Ponce et al., 2011). By contrast, high *FatB* transcription was observed in the developing coffee (*Coffea arabica*) endosperm, cotton (*Gossypium hirsutum*) embryo, and Arabidopsis flower, which contain approximately 40%, 25%, and 27% palmitic acid, respectively (Pirtle et al., 1999; Dörmann et al., 2000; Joët et al., 2009). These few studies therefore suggest that a high 16:0 content could depend on the up-regulation of *FatB* in developing lipid-rich tissues. In plants that store MCFA, studies with California bay (*Umbellularia californica*) and *Cuphea* species demonstrated that the premature cleavage of the acyl chain from ACP is operated by additional specialized FatB thioesterases (Pollard et al., 1991; Voelker and Kinney, 2001). Although the role of acyl-ACP thioesterases in the determination of the plant FA composition appears unquestionable, knowledge about how the transcription of the different *FatA* and *FatB* genes is coordinated during oil biosynthesis remains poorly understood.

Specialized isoforms of other enzymes of the FA and TAG biosynthetic pathways are implicated in the accumulation of MCFA (Voelker and Kinney, 2001). Additional ketoacyl-ACP synthases (KAS) dedicated to MCFA elongation, termed KAS IV (Dehesh et al., 1998), were identified in various *Cuphea* species (Slabaugh et al., 1998). Regarding TAG assembly in the ER, early biochemical studies carried out in palm (*Butia capitata*, *Syagrus cocoides*, and coconut [*Cocos nucifera*]) and *Cuphea* spp. seeds on the enzyme properties involved in the three acylations of glycerol revealed the possible concerted action of specialized glycerol-3-P-acyltransferase (GPAT), lysophosphatidic acid acyltransferase (LPAAT), and diacylglycerol acyltransferase (DGAT) enzymes in MCFA-producing plants (Sun et al., 1988; Bafor and Stymne, 1992; Laurent and Huang, 1992; Wiberg et al., 1994; Davies et al., 1995). However, most studies on oil synthesis in MCFA-producing plants were based on biochemical approaches, and the importance of transcriptional regulation in the synthesis of MCFAs and their incorporation in TAG is less known.

As illustrated above with FatB and KAS enzymes, several isozymes may catalyze each step of FA and TAG synthesis. The question of which gene copies are involved in oil biosynthesis in oil crops is a crucial issue. Using the advantages of Next Generation Sequencing technologies for transcriptional profiling in plants with limited genomic resources, a recent study demonstrated that developing oil seeds of four species with no close evolutionary relationships preferentially use the same orthologous copy for several biosynthetic steps (Troncoso-Ponce et al., 2011). In most cases, the copy predominantly expressed in the four species was also identical to that employed in Arabidopsis developing seeds. This notable finding suggests the conservation of a common set of isoforms for seed storage lipid synthesis throughout plant evolution. The extent to which this phenomenon determines tissue specific lipid synthesis within a single species is less known. In the developing barley (*Hordeum vulgare*) seed, certain lipid-related enzymes were encoded by two paralog genes, one with preferential expression in the embryo and the other with preferential expression in the endosperm (Neuberger et al., 2008). The lipid-rich perisperm and endosperm of the coffee seed employ two distinct paralog genes in most steps that occur in the ER, whereas only one gene copy was found to be involved in the reactions that take place in the plastid (Joët et al., 2009). However, to our knowledge, the limited number of studies that exemplified possible transcriptional specialization among tissues did not investigate the relation to lipid composition.

The search for factors controlling quantitative features of oil accumulation is also of fundamental importance. In particular, our knowledge of how carbon is channeled to FA synthesis in the plastid and how the plastidial FA biosynthetic machinery is activated remains incomplete (Schwender and Ohlrogge, 2002; Alonso et al., 2007; Allen and Young, 2013). Transcriptomic and proteomic studies of developing oilseeds revealed that most glycolysis-related genes are up-regulated in a coordinated manner at the onset of lipid synthesis, suggesting that glycolysis might be regulated at the transcriptional level in plant tissues that accumulate oil (Hajduch et al., 2006; Troncoso-Ponce et al., 2011). However, unraveling glycolysis regulation might be particularly challenging in plants because

of the occurrence of two parallel pathways in the cytosol and the plastid (Plaxton, 1996). Metabolic flux analysis showed limitations to resolve this aspect because of the rapid exchange of labeled glycolytic intermediates between plastidial and cytosolic compartments (Schwender et al., 2003). In this context, quantification of transcripts and/or proteins involved in cytosolic and plastidial glycolysis during tissue development may make it possible to gain insight into their relative contribution to the provision of precursors for oil biosynthesis (Houston et al., 2009).

The identification of the transcription factor WRINKLED1 (WRI1), a member of the APETALA2 (AP2)/ETHYLENE RESPONSE FACTOR family, constituted a key milestone in the understanding of oil synthesis regulation in seeds (Focks and Benning, 1998). The Arabidopsis *wri1* mutant exhibits a drastic decline in seed oil accumulation and lower transcript levels for several steps of plastidial glycolysis and FA synthesis (Ruuska et al., 2002; Cernac and Benning, 2004; Baud et al., 2007). In Arabidopsis, *WRI1* functions downstream of LEAFY COTYLEDON2 (LEC2; Baud et al., 2007), and possibly of LEC1 (Mu et al., 2008) and FUS3 (Yamamoto et al., 2010), three master regulators of Arabidopsis seed maturation. Recently, two maize (*Zea mays*) orthologs of *AtWRI1* (*ZmWRI1a* and *ZmWRI1b*) exhibited up-regulation during seed development and complemented the Arabidopsis *wri1* mutant (Pouvreau et al., 2011). Transcriptome analysis of the developing oil palm mesocarp revealed that a *WRI1* gene was massively transcribed at the onset of oil accumulation and coregulated with FA biosynthetic genes, suggesting WRI1 may also regulate FA synthesis in nonseed tissues (Tranbarger et al., 2011). *WRI1* transcript abundance was about 50-fold higher in the oil palm mesocarp than in that of date palm (*Phoenix dactylifera*), which does not store oil (Bourgis et al., 2011). However, orthologs of *AtWRI1* were not massively transcribed in all developing oil seed tissues studied so far. For instance, *WRI1* peak transcript abundance was very low in the developing embryo of *Tropaeolum majus* and endosperm of *Euonymus alatus* (Troncoso-Ponce et al., 2011), suggesting that the relationships between *WRI1* transcription and oil accumulation need to be clarified in a more substantial number of species and tissues.

In addition to the mesocarp and the endosperm, our preliminary histological and biochemical observations revealed that mature oil palm embryos also store significant amounts of lipids with a high proportion of polyunsaturated FAs (PUFAs). Furthermore, dramatic changes in FA composition have been reported during the development of both the endosperm and the mesocarp (Oo et al., 1986; Wiberg and Bafor, 1995). Some of the regulatory features that lead to the outstanding oil and carotenoid content of the oil palm mesocarp were recently revealed through 454 pyrosequencing-based transcriptome analysis (Tranbarger et al., 2011; Bourgis et al., 2011). In this work, we used a similar transcriptomic approach to decipher lipid biosynthesis in the oil palm embryo and endosperm. Transcriptome comparison of the three oil-storing tissues of oil palm, in combination with their FA profiling during development, provides insight into the mechanisms that govern variations in oil composition. Finally, an agroinfiltration system in *Nicotiana benthamiana* leaves was used to validate some of the candidates potentially involved in these differences.

RESULTS

Stages of Development and Lipid Accumulation in the Three Lipid-Rich Tissues of Oil Palm

Fruits completed their development and maturation in 160 d under the experimental conditions used. At about 50 d after pollination (DAP), the endocarp (shell) started to harden but the endosperm was liquid and could be sampled from 70 DAP when it turned gelatinous. Between 70 and 120 DAP, the endosperm solidified and accumulated lipids massively (+143 mg per seed on average), through combined major increases in dry mass (DM) and lipid content (% DM; Fig. 1A). Between 70 and 100 DAP, major changes in the FA composition of total lipids occurred (Table I). On the whole, there was a significant increase in (C8–C14) and decrease in long-chain (C16–C20). The most noticeable changes concerned the percentage of 18:1, which dropped from 30% to 11%, and that of lauric acid (12:0), which showed a major increase up to 54%. After 120 DAP, the amount of oil in the endosperm continued to increase, but at a much lower rate than during the early stages of development (+42 mg per seed; Fig. 1A), and its FA composition did not exhibit any important change (Table I). In the mature endosperm, MCFA represented 73% of total FA. Confocal microscopy analysis revealed that lipid droplets (5–20 μm in diameter) occupy the majority of the cell volume (Fig. 1C).

In oil palm, the embryo represented 0.4% of the mature seed dry mass only (the average dry mass at maturity was 1.4 and 396 mg for the embryo and the endosperm, respectively). Embryos were large enough to be easily collected using a stereomicroscope from 85 DAP onward. In contrast with the endosperm, which stored most of its oil in the early stages of development, the embryo displayed a continuous accumulation of lipids throughout its development but at a moderate rate (Fig. 1B). Very few changes in the FA composition of total lipids were observed in developing embryos (Table I). Myristic (14:0), 16:0, 18:1, and linoleic (18:2) acids only varied significantly during development and these variations were quantitatively moderate. The most important changes were a decrease in 18:2 content from 29% to 21% and an increase in the percentage of 18:1 from 29% to 37%. Oil palm embryos, however, showed a peculiar FA composition at maturity since they displayed high levels of 16:0, 18:1, and 18:2 (25%–37%) together with a significant proportion of MCFA (7%). Total lipids represented up

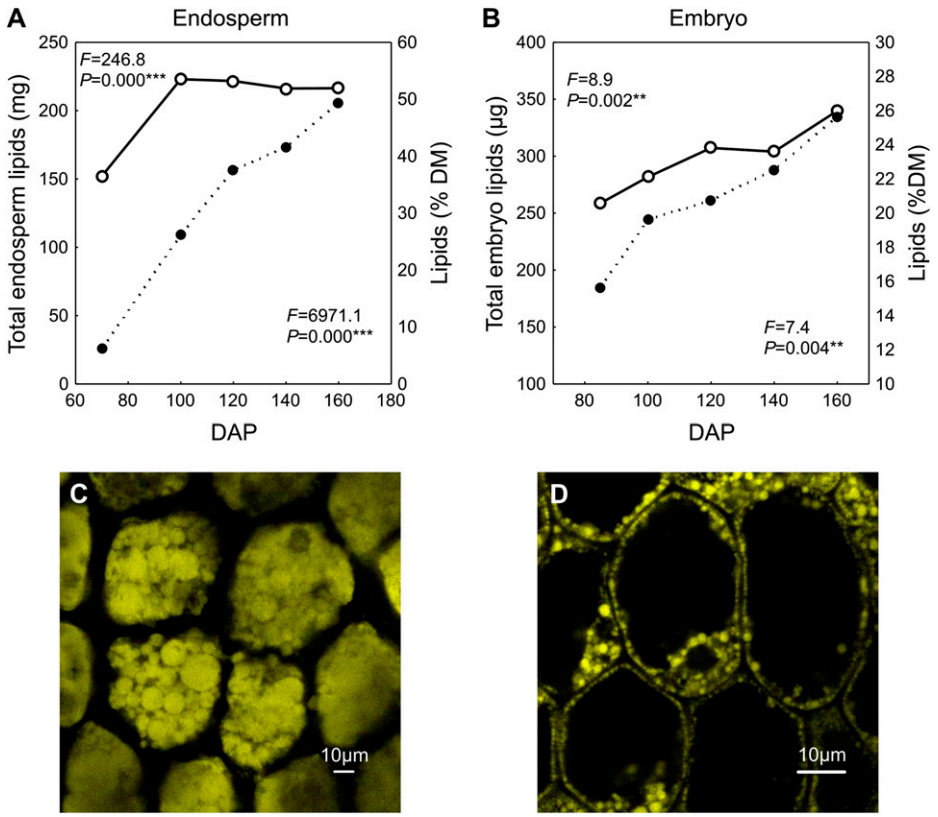

Figure 1. A and B, Patterns of oil accumulation in the developing endosperm (A) and embryo (B) of oil palm (DAP). Lipid content values are expressed as total lipid amounts (mg or μg; black circles) and % DM (white circles). The significance of the effect of the developmental stage was tested by ANOVA (*F* and *P* values). C and D, Confocal microscopy of lipids in the mature endosperm (C) and embryo (D) using Nile red staining.

to 27%DM in mature embryos and droplets were present throughout the periphery of the cells (approximately 2 μm in diameter; Fig. 1D).

The pattern of oil accumulation in the mesocarp was described in a previous study using the same fruit samples (Tranbarger et al., 2011). It showed a major increase in oil content from 120 DAP onward. In this work, we observed substantial changes in the FA composition of total mesocarp lipids at the same stage of development (Table I). At 120 DAP, the proportion of PUFA declined considerably (from 38%–11%), whereas that of 18:1, and to a lesser extent that of 16:0, increased significantly. In the mature mesocarp, 16:0 and 18:1 predominated, representing approximately 40% of total FA, respectively.

Developmental Coordination of FA Synthesis Gene Transcription

After clustering and assemblage of high quality sequence reads, only contigs represented by a minimum total of 20 reads per million were retained for further analyses. Using this criterion, a total of 6,828, 5,281, and 7,968 contigs (Supplemental Data Sets S1–S3) were obtained in the embryo, the endosperm, and the mesocarp, respectively (Table II). Using corresponding Arabidopsis sequences (Li-Beisson et al., 2013), at least one contig was identified in each transcriptome for almost all of the lipid-related enzymes (or subunits) studied (Supplemental Data Set S4). Read amounts associated with each contig at each stage of development were then analyzed using Audic-Claverie (AC) and False Discovery Rate (FDR) statistics. This enabled the identification of 1,483, 2,175, and 2,629 contigs differentially expressed during development in the embryo, the endosperm, and the mesocarp, respectively, i.e. contigs that exhibited a highly significant difference in read abundance ($P = 0.01$) for at least one stage transition. The proportion of FA synthesis enzymes represented by at least one differentially expressed contig (DEC) was very high in the endosperm (15/19) and in the mesocarp (16/20), but only moderate in the embryo (6/19), suggesting a lower developmental control of FA synthesis gene transcription in this tissue. For the three tissues, the number of ER reactions with at least one DEC was very low, which indicates weak developmental transcriptional regulation of TAG assembly in the ER in comparison with de novo FA synthesis in the plastid.

Within each tissue, Hierarchical Clustering Analysis (HCA) was then used to group DEC according to their transcription profile. This allowed classifying DEC in four or five major clusters, depending on the tissue, each divided into three to 10 subclusters (e.g. Supplemental Fig. S1 for the endosperm). Almost all DECs involved in FA synthesis were grouped in the same cluster (termed A_a) in the developing endosperm (Table II), with the exception of those encoding the E3 component of pyruvate dehydrogenase (PDH), long-chain acyl-CoA synthetase (LACS) and stearate desaturase (SAD) classified

Table I. *Fatty acid composition (w/w) of the developing endosperm, embryo, and mesocarp of oil palm (DAP). The significance of the effect of the developmental stage was tested by ANOVA (F and P values; *, P < 0.05; **, P < 0.01; ***, P < 0.001).*

Tissue	DAP	C8:0	C10:0	C12:0	C14:0	C16:0	C18:0	C18:1ω9	C18:1ω7	C18:2	C18:3	Others
Endosperm	70	2.7	2.3	32.9	11.3	9.6	2.6	30.3	0.3	7.4	0.0	0.4
	100	4.7	4.3	54.3	14.7	6.3	1.7	11.4	0.1	2.5	0.0	0.2
	120	4.8	4.3	53.9	15.6	6.7	1.7	10.8	0.1	1.9	0.0	0.2
	140	4.9	4.2	51.3	16.2	7.7	2.1	11.4	0.1	2.0	0.0	0.2
	160	4.1	3.7	49.0	16.1	8.2	2.3	13.9	0.1	2.3	0.0	0.2
	F	10.5	7.9	20.3	32.0	6.4	4.6	47.7	93.0	89.0		
	P	0.001	0.003	0.000	0.000	0.008	0.023	0.000	0.000	0.000		
		**	**	***	***	**	*	***	***	***		
Embryo	85	0.1	0.1	2.1	1.2	27.0	3.9	29.5	5.6	28.8	0.1	1.6
	100	0.4	0.3	3.4	1.5	24.9	3.8	35.3	5.1	23.9	0.1	1.4
	120	0.4	0.3	5.7	3.1	23.3	4.8	34.7	4.8	21.3	0.1	1.3
	140	0.4	0.3	5.8	3.1	23.7	4.1	34.8	5.0	21.5	0.1	1.2
	160	0.2	0.2	4.2	2.3	24.7	4.2	37.1	4.4	21.2	0.1	1.4
	F	2.7	2.8	2.6	3.6	6.4	2.0	4.7	1.2	25.4	0.8	
	P	0.084	0.080	0.096	0.041	0.006	0.159	0.018	0.347	0.000	0.552	
					*	**		*		***		
Mesocarp	70	0.1	0.2	1.2	1.7	36.6	4.2	14.5	0.6	26.0	12.5	2.6
	100	0.2	0.3	2.4	2.1	34.2	3.5	16.4	0.8	26.6	10.9	2.7
	120	0.0	0.0	0.0	0.9	45.5	4.3	36.7	0.7	10.5	0.6	0.7
	140	0.0	0.0	0.2	1.7	42.3	6.7	39.6	0.4	8.0	0.4	0.8
	160	0.0	0.0	0.1	1.7	42.0	7.1	39.2	0.4	8.4	0.3	0.8
	F	3.7	5.7	3.8	3.4	51.4	97.7	334.8	29.3	534.5	1037.0	
	P	0.049	0.015	0.045	0.057	0.000	0.000	0.000	0.000	0.000	0.000	
		*	*	*		***	***	***	***	***	***	

in clusters B_a, C_a, and E_a, respectively. Moreover, most of cluster A_a DEC belonged to subclusters A_a1 and A_a6 (Supplemental Fig. S2). DECs belonging to cluster A_a displayed maximal transcription at 70 to 85 DAP, the period for maximal oil deposition in the endosperm (Fig. 1), demonstrating a remarkable transcriptional coordination of the core FA synthesis machinery in this tissue. This was already observed in the oil palm mesocarp at 120 DAP (Tranbarger et al., 2011) with 17 DEC involved in FA synthesis that coclustered in cluster B_m (Table II). Two mesocarp FA synthesis DECs that were not classified into cluster B_m also encoded a SAD and a LACS.

Tissue Transcriptional Specialization through Paralog Preferential Expression

For each step of the pathways leading to the accumulation of TAG, the comparison of the three transcriptomes

Table II. *Pyrosequencing, contig assembly, AC and FDR tests, and HCA statistics*

The FA synthesis enzymes investigated were the 20 plastidial enzymes described in Fig. 3. All ER proteins (excluding oleosins and caleosins) described in Fig. 3 were considered for statistics. HCA results detail the distribution of the DECs involved in fatty acid synthesis (cluster names and numbers of DEC per cluster).

Statistics	Embryo	Endosperm	Mesocarp
No. of reads	1,049,224	1,002,153	587,621
Average read length	309	307	380
No. of high-quality reads	848,064	909,467	528,234
No. of contigs	58,323	42,407	29,034
No. of contigs with ≥ 20 reads per million reads	6,828	5,281	7,968
No. of synthesis enzymes represented by ≥ 1 contig (20 functions examined)	19	19	20
No. of ER enzymes represented by ≥ 1 contig (10 functions examined)	10	7	10
AC and FDR tests			
No. of DECs	1,483	2,175	2,629
No. of synthesis enzymes represented by ≥ 1 DEC	6	15	16
No. of ER enzymes represented by ≥ 1 DEC	2	2	3
HCA			
DEC involved in synthesis	$B_e = 4$ $D_e = 1$ $E_e = 1$	$A_a = 14$ $B_a = 1$ $C_a = 1$ $E_a = 3$	$B_m = 17$ $C_m = 2$

allowed for the determination of the number of paralogous genes transcribed in oil palm independent of the tissue. Tissue transcriptional specialization was then investigated using the number of paralogs identified per enzymatic reaction and, when more than one copy was found, the transcriptional status of each paralog in each tissue. Venn diagrams were used to depict the distinct situations observed (Fig. 2).

The simplest case corresponded to enzymes for which a single gene was found in the three transcriptomes (Venn diagrams with green-colored central sections). Such enzymes represented most of the biosynthetic steps and were involved in both de novo formation of acyl chains (α-subunit of E1 component of PDH; E3 component of PDH; carboxyltransferase β-subunit and biotin carboxyl carrier protein subunit of the acetyl-CoA carboxylase complex; malonyl-CoA:ACP malonyltransferase; hydroxyacyl-ACP dehydrase; ketoacyl-ACP reductase; enoyl-ACP reductase; KAS II) and TAG assembly (GPAT; 1-acylglycerol-3-P acyltransferase, LPAAT of classes A and B; phospholipid:diacylglycerol acyltransferase [PDAT]; acyl-CoA:diacylglycerol acyltransferase of type 2). A single gene was also found in the three transcriptomes for ω6-desaturase (FAD2). A second case, also showing no tissue transcriptional specialization, corresponded to proteins for which several paralogs were detected but the most transcribed paralog was the same in the three tissues (Supplemental Table S1). Proteins of this second group (with a yellow-colored Venn diagram in Fig. 2) were all plastidial and included two subunits of the acetyl-CoA carboxylase complex, the β-subunit of the E1 component of PDH, KAS I and KAS III, SAD, and ACPs.

A first mode of transcriptional specialization consisted of genes that were not detected in one or two of the three oil-storing tissues analyzed (Venn diagrams with red-colored sections, Fig. 2). FatA transcripts accumulated in the mesocarp only. Genes encoding ω3-desaturase (FAD3) and diacylglycerol cholinephosphotransferase (CPT) were expressed in the mesocarp and the embryo only. It is worth noting that of the seven oleosin gene transcripts identified in both the embryo and the endosperm, none were expressed in the mesocarp.

Finally, transcriptional specialization through tissue-specific paralog preferential use concerned a reduced number of enzymes (Venn diagrams with blue-colored sections, Fig. 2). Among enzymes for which distinct gene copies were preferentially expressed in the three tissues (Supplemental Table S1), one participates to acetyl-CoA production (E2 component of PDH), two are involved in the release of nascent FA from the plastid to the ER (FatB thioesterases and LACS), and the last two participate to the last acylation of the glycerol backbone to produce TAG (DGAT1 and 1-acylglycerol-3-phosphocholine acyltransferase [LPCAT]). In the cases of FatB, LACS, and DGAT1, the main paralog in the mesocarp was different from that in the endosperm and the embryo. For LPCAT, the copy transcribed in the endosperm was different from that used in the mesocarp and the embryo. This approach thus enabled us to list the enzymatic reactions (FATA, FATB, LACS, CPT, FAD3, DGAT1) that potentially determine the different FA compositions of the three TAGs accumulating oil palm tissues.

Tissue-Specific Transcriptional Regulation of Acyl-ACP Thioesterases

To ascertain the classification of the four acyl-ACP thioesterase genes identified, a phylogenetic tree was generated using their deduced amino acid sequence and that of various known plant FatA and FatB sequences (Supplemental Fig. S3). This approach confirmed the existence of three *FatB* paralogs, thereafter termed *EgFatB1*, *EgFatB2*, and *EgFatB3*, and one *FatA* gene in the transcriptomes of developing oil palm fruit and seed tissues. The transcription of *EgFatA* in the mesocarp was in agreement with the high proportion (39%) of 18:1 of the mesocarp oil (Fig. 3). By contrast, no *EgFatA* transcripts were detected in the embryo and the endosperm, while both tissues accumulated significant amount of unsaturated FA. The percentage of unsaturated FA in the embryo (63%) was even higher than that of the mesocarp. This result indicates that at least one of the FatB isoforms of oil palm hydrolyzes 18:1-ACP very efficiently. Among the three *FatB* paralogs identified, the level of transcription of *EgFatB3* was the most proportionally related to MCFA accumulation (Fig. 3). This paralog was massively transcribed (peak value of 560/200,000 reads at 85 DAP; Supplemental Fig. S2) in the endosperm, which contained 73% MCFA at maturity, moderately transcribed in the embryo (57/200,000 reads) whose MCFA content was 7%, and not expressed in the mesocarp, which did not contain MCFA. By contrast, the transcription profiles of *EgFatB1* and *EgFatB2* in the three tissues do not make it possible to ascertain their respective roles at the branch point between C16 release and elongation to C18.

Variations in TAG Assembly and PUFA Enrichment between Tissues

Two main routes of TAG assembly are likely to coexist in oil palm tissues, one leading to the accumulation of TAG acylated with MCFA and the other one to TAG rich in palmitate, oleate, and PUFA (Fig. 4). Because a single gene was transcribed in the three tissues for GPAT activity, the first acylation on the *sn*-1 position of the glycerol backbone appears to be common to both routes. This suggests that the oil palm GPAT efficiently uses all types of acyl-CoA, independent of length and unsaturation status. The transfer of acyl-CoA at the second position of glycerol is catalyzed by LPAATs, which separate in two classes of genes termed LPAAT-A and LPAAT-B (Frentzen, 1998). Genes of both classes (Supplemental Fig. S4) were significantly transcribed in the endosperm and the embryo during oil deposition, whereas only

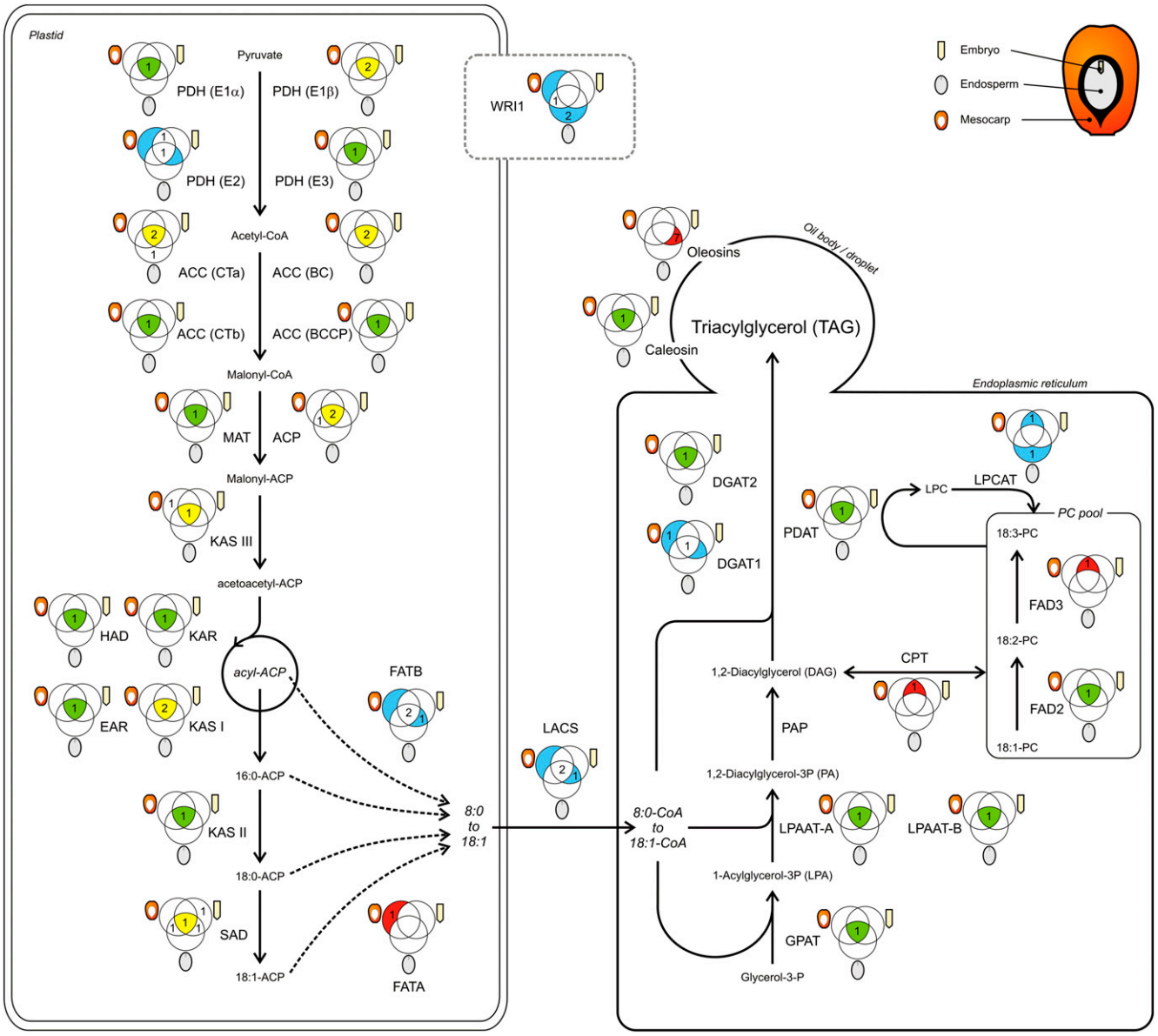

Figure 2. Tissue transcriptional specialization of lipid-related genes in the developing embryo, endosperm, and mesocarp of oil palm. For each enzyme or protein, figures given within sections of the Venn diagram indicate the numbers of tissue-specific or shared gene copies found in the transcriptome of the three tissues. Colors are used to highlight the four distinct cases identified regarding transcriptional specialization and to specify the main paralog used by each tissue: (1) a single gene was found in the three transcriptomes (green-colored central section); (2) several paralogs were detected but the most transcribed paralog was the same in the three tissues (yellow-colored central section); (3) genes that were not transcribed in one or two of the three oil-storing tissues analyzed (red-colored sections); (4) distinct paralogs were preferentially used in the three tissues (blue-colored sections). ACC (BC), Biotin carboxylase subunit of heteromeric acetyl-CoA carboxylase (ACCase); ACC (BCCP), biotin carboxyl carrier protein of heteromeric ACCase; ACC (Ctα), carboxyltransferase α-subunit of heteromeric ACCase; ACC (Ctβ), carboxyltransferase β-subunit of heteromeric ACCase; EAR, enoyl-ACP reductase; FAD2, ω-6 desaturase; FAD3, ω-3 desaturase; FATA, acyl-ACP thioesterase A; FATB, acyl-ACP thioesterase B; HAD, hydroxyacyl-ACP dehydrase; KAR, ketoacyl-ACP reductase; MAT, malonyl-CoA:ACP malonyltransferase; PAP, phosphatidate phosphatase; PDH (E1α), subunit α of E1 component of PDH complex; PDH (E1β), subunit β of E1 component of PDH complex; PDH (E2), E2 component of PDH complex; PDH (E3), E3 component of PDH complex.

transcripts encoding LPAAT-A accumulated in the mesocarp. Because EgLPAAT-B closely grouped with CnLPAAT-B of coconut (Supplemental Fig. S4), which was shown to efficiently transfer medium-chain acyl-CoA (Knutzon et al., 1995), one may assume that EgLPAAT-B primarily participates in the production of diacylglycerols (DAGs) esterified with MCFA in the developing endosperm and embryo (Fig. 4).

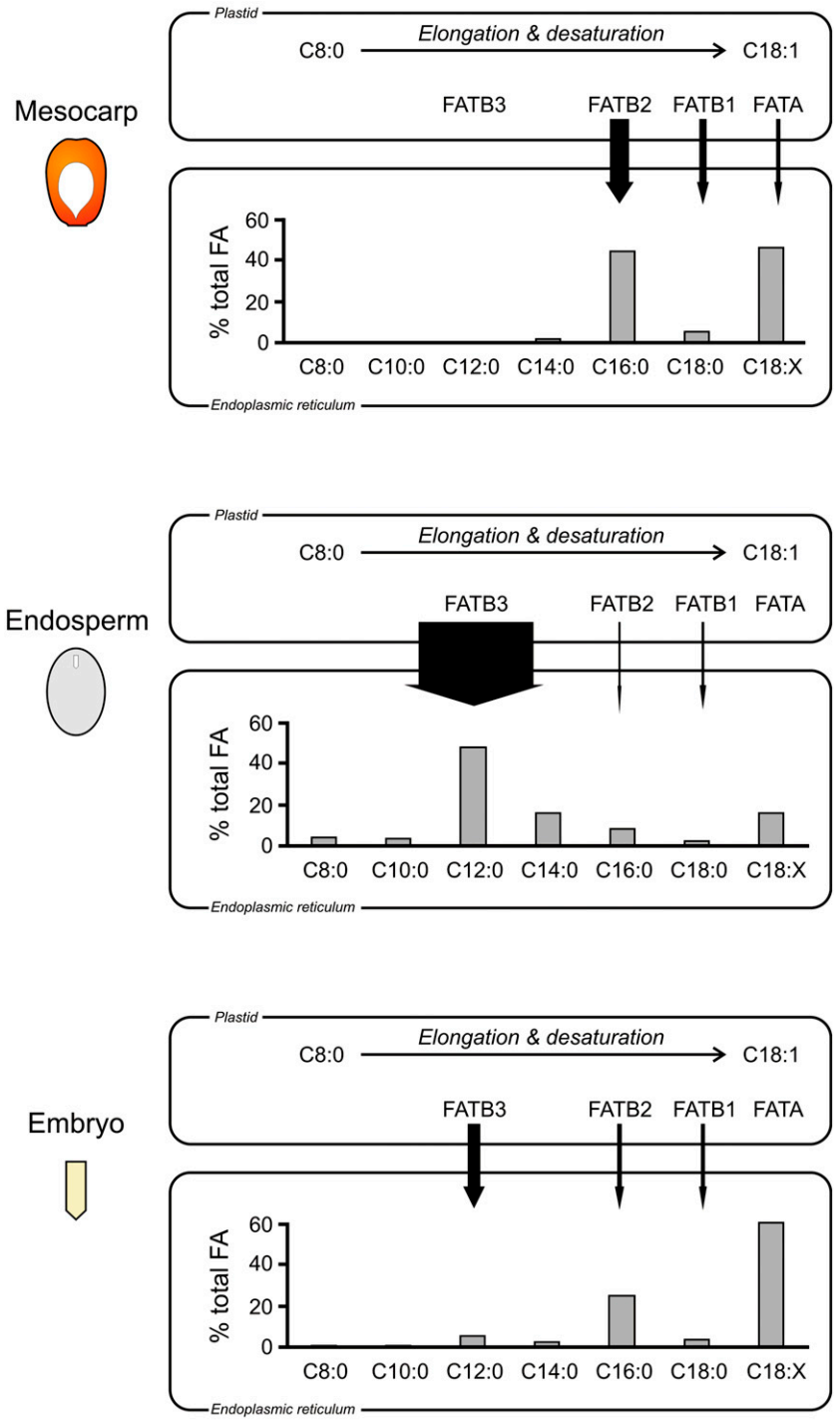

Figure 3. Fatty acid profile of mature tissues and peak transcript abundance, as indicated by the width of arrows that symbolize fluxes of nascent fatty acids from the plastid to the endoplasmic reticulum, of the three genes encoding FatB acyl-ACP thioesterases and of the FatA gene. The width of each arrow is strictly proportional to the level of gene expression. C18:X indicates the sum of C18:1, C18:2, and C18:3 percentages. [See online article for color version of this figure.]

Since acyl-CoAs resulting from FA synthesis are saturated or monounsaturated, the incorporation of PUFA in TAG requires the involvement of complementary pathways. A first possible route involves DAG-phosphatidylcholine (PC) interconversion. DAG species formed through the Kennedy pathway are converted to PC through CPT (Figs. 2 and 4) or phosphatidylcholine:diacylglycerol cholinephosphotransferase (PDCT) activity (Lu et al., 2009). Oleate esterified to the resulting PC at the *sn*-2 position can then be desaturated to 18:2 by FAD2 and the resulting 18:2 can be further desaturated to 18:3 by FAD3. The reversibility of the reactions catalyzed by CPT and PDCT enables to enrich DAG in PUFA. No contig was identified for PDCT in the three tissue transcriptomes. By contrast, the level of transcription of *EgCPT* was clearly associated with the proportion of PUFA in mature tissues. It was massively

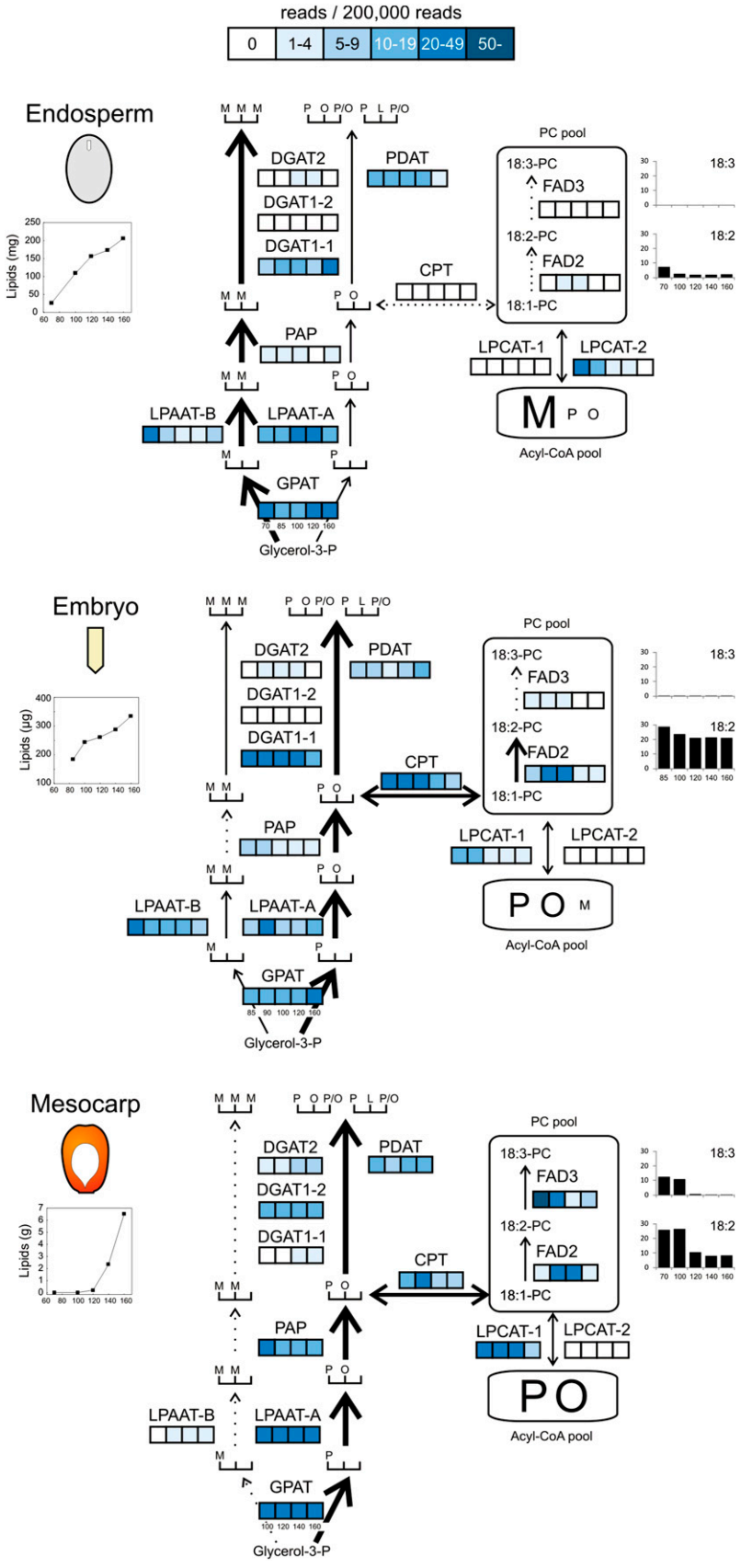

Figure 4. TAG assembly in the three oil-storing tissues of oil palm. Gene expression levels at the various developmental stages analyzed are indicated with colored bars (DAP of each stage is given under the GPAT bar). For each developmental stage, colors specify the number of reads per 200,000 reads. Letters indicated in the acyl-CoA pools and triacylglycerol molecules correspond to major fatty acids as expected from chemical profiling. M, MCFA; P, palmitic acid; O, oleic acid; L, linoleic acid. Enzyme abbreviations are given in the legend of Fig. 2. PAP, Phosphatidate phosphatase.

transcribed in the embryo which contained 21% PUFA at maturity (Fig. 4; Table I). The mesocarp PUFA content was lower (8%) than that of the embryo and the level of transcription of *EgCPT* in the mesocarp was correspondingly moderate during oil deposition. Finally, no CPT transcript was consistently detected in the endosperm with its very low PUFA percentage. About 75% of mesocarp 18:2 is at the *sn*-2 position of TAG (Gouk et al., 2012). This proportion is in agreement with an enrichment of TAG in PUFA through PC-DAG interconversion. The transcription profile of *EgFAD2* and *EgFAD3* were also highly consistent with the PUFA content of the three tissues (Fig. 4). For instance, the expression of genes encoding the two desaturases was very low or nil in the endosperm. In the mesocarp, the abrupt decline of the 18:3 content that occurred at 120 DAP coincided with a significant decrease in *EgFAD3* transcription.

A second possible route consists of the transfer of PUFA from PC to DAG by the PDAT enzyme to form lyso-PC and TAG. *EgPDAT* was expressed moderately in the three oil palm tissues (Fig. 4). Therefore, differences in PUFA content of the three tissues cannot be explained by the transcription of *EgPDAT*. It is possible that PDAT activity contributes to the acylation of the low proportion of PUFA that are not found at the *sn*-2 position of TAG. Two tissue-specific paralogous genes were identified for LPCAT (Figs. 2 and 4), whose activity is necessary to regenerate PC from lyso-PC produced by PDAT. *EgLPCAT-1* was transcribed in the mesocarp and the embryo, whereas transcripts of *EgLPCAT-2* accumulated only in the endosperm during peak oil deposition. Alternatively, the two LPCAT isoforms could play a role in the exchange of FA between the pool of PC and that of acyl-CoA through the "acyl editing" mechanism (Bates et al., 2009). This process constitutes the third potential route for PUFA incorporation into TAG. In the endosperm, the proportion of 18:2 was very low but not nil. Because there was no CPT activity in this tissue, acyl editing could play a significant role in the incorporation of 18:2 in TAG.

The third acylation that converts DAG into TAG may be catalyzed by PDAT, as described above, and DGAT enzymes of type 1 and type 2. Two DGAT1 paralogs and one DAGT2 were identified in the transcriptomes of the three oil-accumulating tissues of oil palm (Supplemental Fig. S5). Transcription of *EgDGAT2* was equally low in the three tissues (Fig. 4). By contrast, together with LPCAT, DGAT1 was the second ER enzyme showing tissue-specific paralog preferential transcription (Fig. 2). Transcripts of *EgDGAT1-1* accumulated in the endosperm and in the embryo only, whereas *EgDGAT1-2* was exclusively transcribed in the mesocarp (Fig. 4). Because the endosperm massively accumulated TAG that contained only MCFA, the EgDGAT1-1 isoform is necessarily able to efficiently transfer MCFA at the *sn*-3 position of glycerol.

The Three Oil-Storing Tissues of Oil Palm Display Transcriptional Divergence of WRI1 Paralogs

Ten contigs, termed *EgAP2-1* to *EgAP2-10*, potentially encoding transcription factors of the AP2 family were identified in the transcriptomes of the three oil palm tissues analyzed. Phylogenetic analysis of their deduced amino acid sequences (double AP2 domains), in combination with those from other plants chosen to represent the three clades of this family, revealed that three of these 10 contigs (*EgAP2-2*, *EgAP2-3*, and *EgAP2-4*) grouped within the clade WRINKLED (Fig. 5A). The classification of these three contigs (full sequences) was further investigated through a second analysis using the four WRINKLED members of Arabidopsis (To et al., 2012), the two paralogous *WRI1* copies of maize (Pouvreau et al., 2011), and *WRI1* sequences from rape (*Brassica napus*; Liu et al., 2010) and rice (*Oryza sativa*; Ye et al., 2004). The three oil palm sequences clearly grouped together with other WRI1 sequences within a branch that contained copies of other monocots (Fig. 5B). The three oil palm sequences therefore appeared to be three paralogous copies of *WRI1* and are hereafter referred to as *EgWRI1-1* to *EgWRI1-3*. Besides, it is worth noting that only one homolog of *ZmVP1/AtABI3* was significantly expressed in the developing embryo and endosperm (Supplemental Table S1). No sequences with significant similarity to *AtLEC2* and *AtFUS3* were found in the embryo and endosperm transcriptomes. Contigs potentially encoding LEC1-like transcription factors were identified in the transcriptome of both seed tissues but were not in the sets of genes represented by at least 20 reads per million.

None of the three *WRI1* paralogs were transcribed in the embryo, demonstrating that oil deposition does not strictly depend on activation of FA synthesis genes by *WRI1* (Fig. 6). *EgWRI1-1* was massively transcribed in the mesocarp and very poorly transcribed in the endosperm. The major *WRI1* paralog in the endosperm was *EgWRI1-2*, though significant amounts of *EgWRI1-3* transcripts were also detected in this tissue. The transcript profile of *EgWRI1-2* and *EgWRI1-3* in the endosperm perfectly coincided with that of most genes involved in FA synthesis (Supplemental Fig. S2; contigs CL1Contig2848 and CL1Contig4038, respectively) and these two *WRI1* copies grouped with these genes within cluster A_a (Supplemental Fig. S1). We previously observed the same temporal coexpression of FA biosynthetic genes and *EgWRI1-1* in the developing oil palm mesocarp (Tranbarger et al., 2011). Comparison of peak read counts in the three tissues allowed us to investigate possible quantitative associations between transcription levels of *WRI1* copies and FA biosynthetic genes, and finally with the amount of oil accumulated. The mean peak transcription level of genes encoding FA synthesis enzymes correlated with the amount of *WRI1* transcripts, independent of the *WRI1* paralog (Fig. 6). Finally, the oil content of mature tissues also varied with the mean peak expression level of FA biosynthetic genes, suggesting a possible causal

Figure 5. Phylogenetic analysis of the three oil palm WRI1 isoforms. A, Neighbor-joining tree obtained with the 10 oil palm proteins of the AP2 family, termed EgAP2-1 to EgAP2-10, with other transcription factors of this family from Arabidopsis (At), rape (Bn), rice (Os), and maize (Zm). Proteins separated in three clades termed AP2, AINTEGUMENTA-LIKE/PLETHORA (AIL/PLT), and WRINKLED. Deduced amino acid sequences of the double AP2 domains were used for distance analysis. B, Neighbor-joining tree obtained with the three oil palm proteins that grouped in the clade WRINKLED (EgAP2-2, EgAP2-3, and EgAP2-4) with other WRINKLED transcription factors from Arabidopsis (At), rape (Bn), rice (Os), and maize (Zm). Full-length deduced amino acid sequences were used for distance analysis. Numbers on the branches are bootstrap value for 100 replicates.

quantitative relationship between the transcription of *WRI1* and FA synthesis genes and the amount of oil deposited.

Combined Effects of Transient Expression of Oil Palm WRI1 and FatB Paralogs on *N. benthamiana* Leaf TAG Content and FA Profile

To validate the specificity of the three oil palm FatB isoforms, the effect of their transient expression in *N. benthamiana* leaves was measured using several biological replicates. This assay requires the induction of oil synthesis in *N. benthamiana* leaves through infiltration of a *WRI1* gene and is an efficient method for functional screening of lipid-related genes (Wood et al., 2009; Vanhercke et al., 2013). Both *EgWRI1-1* and *EgWRI1-2* induced a severalfold increase in leaf TAG levels in comparison with the control (Fig. 7). TAG content was 0.049%DM in control leaf samples, and 0.425%DM and 0.100%DM in leaf samples infiltrated with *EgWRI1-1* and *EgWRI1-2*, respectively. Infiltration

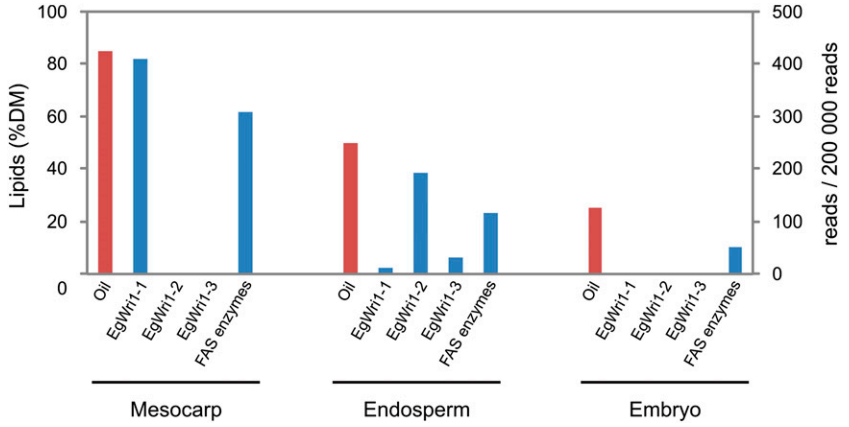

Figure 6. Relationships between amounts of oil (% DM) accumulated in the mesocarp, endosperm, and embryo of oil palm, peak transcription levels of the three *WRI1* paralogs, *EgWRI1-1*, *EgWRI1-2*, and *EgWRI1-3*, and mean peak transcription levels of genes encoding fatty acid synthesis (FAS) enzymes. All genes encoding plastidial enzymes shown in Fig. 3, with the exception of SAD and thioesterase (FatA and FatB) genes, were included in the calculation of mean FAS gene transcription levels. SAD genes were not taken into account because their transcriptional profile did not cocluster with other FAS genes. Because of the outstanding up-regulation of *EgFatB3* in the endosperm (Fig. 4), genes encoding acyl-ACP thioesterases were also discarded. [See online article for color version of this figure.]

with *AtWRI1* provided TAG levels similar to those obtained with *EgWRI1-1* (data not shown). Coinfiltration of *EgWRI1-1* with any of the three *FatB* paralogs of oil palm led to a further increase in the TAG content of *N. benthamiana* leaves, which was about 3 times higher than with infiltration of *EgWRI1-1* alone (Fig. 7). A similar synergistic effect of combining *EgWRI1-2* and *EgFatB3* transient expression was observed in comparison with *EgWRI1-2* alone. These synergistic effects suggest that the transfer of nascent FA from the plastid to the ER is another limiting step in TAG accumulation in *N. benthamiana* leaves. Alternatively, it may be hypothesized that free ACP becomes limiting for FA synthesis when triggered by *EgWRI1* transient expression and that the pool of ACP is regenerated more efficiently when a *FatB* paralog is expressed concomitantly.

Transient expression of *EgWRI1-1* or *EgWRI1-2* alone did not modify extensively the FA composition of TAG accumulated in *N. benthamiana* leaves (Fig. 8). By contrast, coinfiltration with any of the three oil palm *FatB* genes led to major changes in FA composition. Whatever the *FatB* paralog used, the percentage of 18:3 substantially declined from 40% to 20%. A 2-fold decrease in the leaf TAG 18:2 content was also observed. Reciprocally, a major increase in saturated FA was observed with the three oil palm *FatB* genes (Fig. 8). However, while significant levels of MCFA appeared in the FA profile of leaves infiltrated with *EgFatB3*, expression of *EgFatB1* and *EgFatB2* mostly impacted the 16:0 percentage. The extent of increase in 16:0 was similar with *EgFatB1* and *EgFatB2* (i.e. 35%–60%. When leaves were infiltrated with *EgFatB3*, the 16:0 increase was lower (up to 45%), but significant levels of 14:0 (approximately 15%) and small amounts of 12:0 (approximately 1%) accumulated in leaf TAG. These results suggest that, among the three *FatB* paralogs identified in the three oil palm oil-storing tissue transcriptomes, only *EgFatB3* was able to prematurely cleave the elongating acyl-ACP in the plastid. It is worth noting that leaves infiltrated with *EgFatB3* mostly accumulated 14:0 and not 12:0 as expected from the endosperm FA composition. However, such a difference in MCFA composition between a transformed plant and the tissue the MCFA-specific FatB gene was cloned from was observed in many studies (for review, see Dehesh, 2001).

The Mesocarp and the Seed Tissues Employ Different Pathways for the Conversion of Suc to Pyruvate

Differentially expressed contigs related to sugar import and glycolysis predominantly grouped in cluster A in the endosperm, clusters A and B in the embryo, and cluster B in the mesocarp, demonstrating that genes involved in the conversion of Suc to pyruvate are transcriptionally coordinated with those of the core FA biosynthetic machinery during peak oil accumulation (Supplemental Table S1). This enabled a comparison of the three tissues for the mechanisms governing upstream Suc import and cleavage and the contribution of the cytosolic and plastidial parallel routes for the oxidation of hexoses to pyruvate using contig transcription levels at the onset of oil deposition (Fig. 9).

Mechanisms for apoplastic sugar import appeared similar in the endosperm and the embryo, in which hexose transporters were only faintly expressed and no transcripts encoding cell wall invertase were detected (Fig. 9). In these tissues, Suc import seems to primarily operate through Suc transporters and its intracellular cleavage is likely to predominantly rely on the activity of Suc synthase with transcripts that accumulated at high levels in both tissues. By contrast, the mesocarp

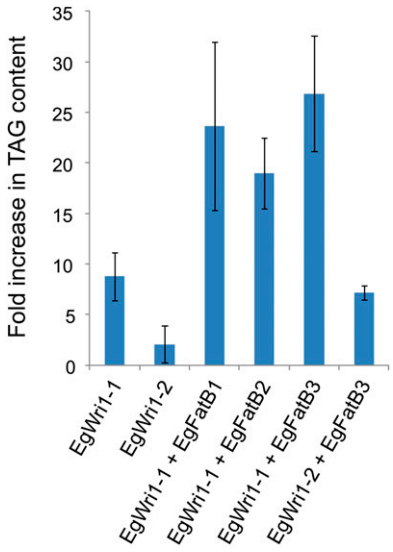

Figure 7. Mean fold increase (over control) in TAG content of *N. benthamiana* leaves infiltrated with two oil palm *WRI1* paralogs, *EgWRI1-1* or *EgWRI1-2*, in combination or not with three oil palm FatB acyl-ACP thioesterase paralogs, *EgFatB1*, *EgFatB2*, and *EgFatB3*. [See online article for color version of this figure.]

exhibited high transcriptional activity for invertase and hexose transporters genes, suggesting that extracellular Suc cleavage was also a substantial source of cellular Glc and Fru in this tissue.

Transcriptional patterns of genes involved in glycolysis were again very similar in the endosperm and the embryo, with a massive accumulation of transcripts for almost all glycolytic enzymes of the cytosolic compartment (>500/200,000 reads), in particular for glyceraldehyde 3-P dehydrogenase (GAPDH) and enolase (ENO), potential main targets for transcriptional control (>1,500/200,000 reads). In the two seed tissues, plastidial glycolytic genes were only slightly expressed, suggesting that most of the carbon flow toward lipid metabolism occurs through cytosolic glycolytic reactions, at least down to phospho*enol*pyruvate (PEP) in the endosperm, at which point carbon is likely imported into plastids and converted into pyruvate. The large accumulation of transcripts for PEP translocator and plastidial pyruvate kinase in this tissue suggests that the last step of glycolysis occurs in plastids. In the embryo, one should also note the massive accumulation of transcripts for the inorganic pyrophosphate (PPi)-dependent phosphofructokinase (PFP) in comparison with the ATP-dependent phosphofructokinase (PFK), and the parallel lack of expression of pyrophosphatase (PPiase) genes, suggesting a role for PFP in the regulation of cytosolic PPi/inorganic phosphate homeostasis.

In the mesocarp, transcripts for early glycolytic enzymes such as Glc phosphate isomerase, PFK, Fru biphosphate aldolase, and GAPDH appeared to accumulate in equal amounts in the cytosol and the plastid, suggesting a tight coordination of glycolysis in both compartments, at least down to 1,3-bisphosphoglycerate (1.3PGA). The massive accumulation of transcripts for upstream plastidial Glc transporter and Glc-6-P/phosphate translocator compared with that observed in the endosperm and the embryo reinforces the hypothesis for a major contribution of plastidial glycolysis in the mesocarp. The contribution of plastidial reactions from 1.3PGA to PEP seems equivocal since

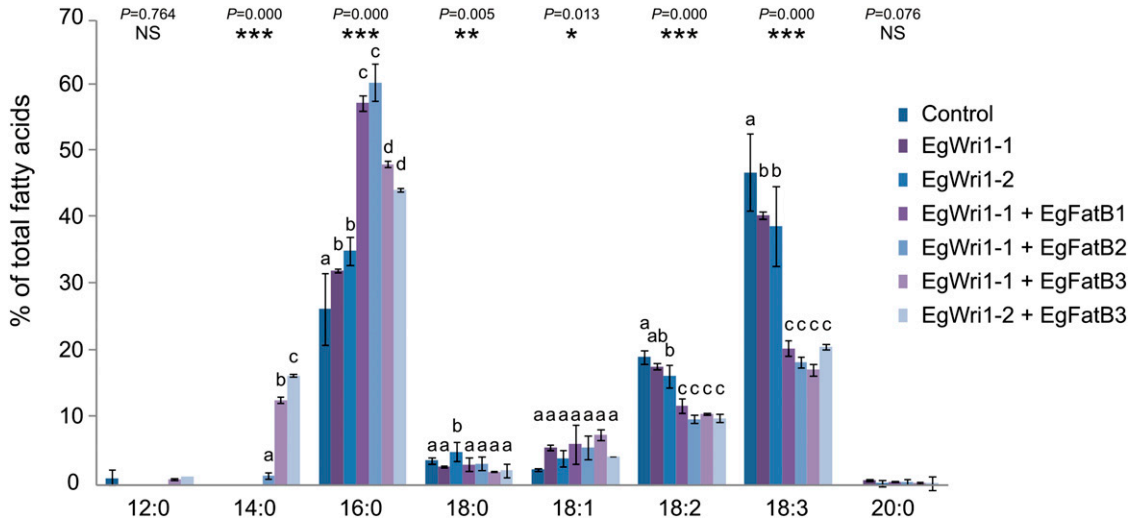

Figure 8. Fatty acid composition of TAGs in *N. benthamiana* leaves infiltrated with two oil palm *WRI1* paralogs, *EgWRI1-1* or *EgWRI1-2*, in combination or not with three oil palm FatB acyl-ACP thioesterase paralogs, *EgFatB1*, *EgFatB2*, and *EgFatB3*. Bars topped by the same letter were not significantly different according to one-way ANOVA (*P* value) and post hoc Newman and Keuls test (analyses were performed for each FA separately). [See online article for color version of this figure.]

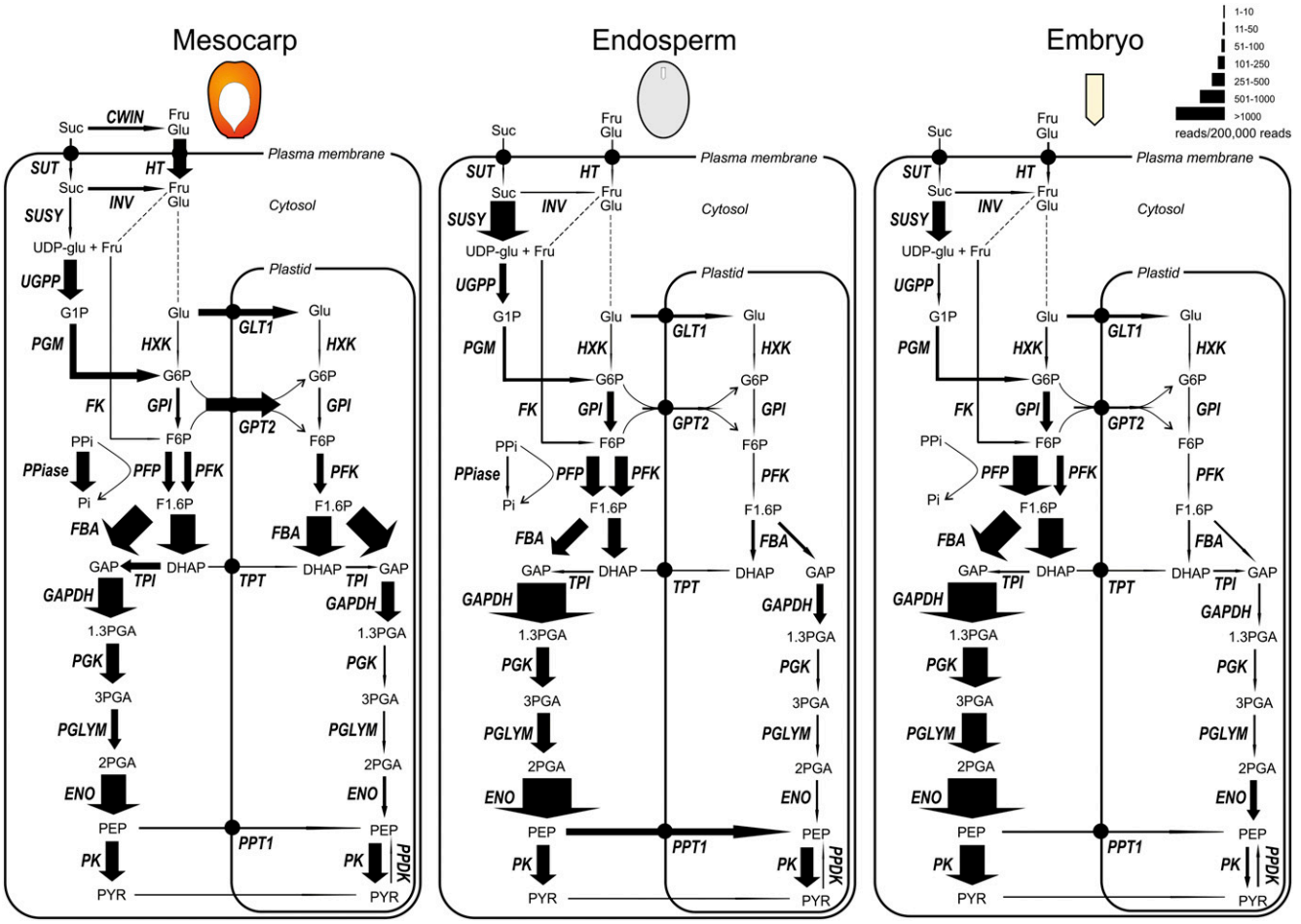

Figure 9. Transcript abundance of enzymes involved in the conversion of Suc to pyruvate in the mesocarp, endosperm, and embryo of oil palm at 120, 70, and 90 DAP, respectively. For each enzyme, the width of the arrow indicates the level of gene expression as described. Read counts of the different isoforms and/or subunits were summed. For simplicity reasons, unidirectional arrows were presented even if most reactions are theoretically reversible (except for reactions catalyzed by hexokinase, phosphofructokinase, and pyruvate kinase). Annotation and read counts for each enzyme are provided in Supplemental Table S1. CWIN, Cell wall invertase; DHAP, dihydroxyacetone-3-P; FBA, Fru-bisphosphate aldolase; FK, fructokinase; F1.6P, Fru-1,6-bisphosphate; F6P, Fru-6-P; GAP, glyceraldehyde 3-P; G1P, Glc-1-P; G6P, Glc-6-P; Glu, Glc; GLT1, Glc transporter; GPI, Glc-phosphate isomerase; GPT2, Glc-6-phosphate/phosphate transporter; HXK, hexokinase; HT, hexose transporter; INV, neutral invertase; PEP, phospho*enol*pyruvate; PFK, phosphofructokinase, PFP, ppi-dependent phosphofructokinase; 2PGA, 2-phosphoglycerate; 3PGA, 3-phosphoglycerate; PGM, phosphoglucomutase; PGI, phosphoglucose isomerase; Pi, inorganic phosphate; PK, pyruvate kinase; PPDK, pyruvate-Pi-dikinase; PPT1, phospho*enol*pyruvate/phosphate translocator; Pyr, pyruvate; SUSY, Suc synthase; SUT, Suc transporter; TPI, triose-P isomerase; UGPP, UDP-Glc pyrophosphorylase. [See online article for color version of this figure.]

the transcription level of the three genes encoding the enzymes involved was very low (phosphoglycerate kinase [PGK], phosphoglycerate mutase [PGLYM], and ENO). Alternatively, the plastidial triose phosphate (triose-P) pool might be shuttled back to the cytosol by triose-P/phosphate translocator (TPT) and followed the downstream steps of the cytosolic pathway. The transcription level of the cytosolic forms of PGK, PGLYM, ENO was very high.

Pathways shown in Figure 9 are theoretically capable of producing the carbon sources alone, reducing equivalents and energy required for FA synthesis. However, glycolytic intermediates, such as Glu-6-P, PEP, and pyruvate may also indirectly provide reducing equivalents and energy through the tricarboxylic acid cycle, malate synthesis, or the pentose phosphate pathway (Schwender et al., 2003, 2006; for review, see Baud and Lepiniec, 2010). Moreover, the Rubisco bypass (Schwender et al., 2004) may also furnish carbon for FA synthesis. However, in the three oil palm tissues analyzed, the transcripts encoding the corresponding enzymes were only slightly expressed, with no clear differences between the three tissues (Supplemental Table S1).

DISCUSSION

The Central Role of Acyl-ACP Thioesterase Transcriptional Regulation

It is generally accepted that the substrate specificity of FatA and FaTB acyl-ACP thioesterases determine to a large extent the FA composition of storage lipids in plants (Pollard et al., 1991; Dörmann et al., 1993; Jones et al., 1995). A second mechanism that may modulate the chain length of FA in TAG is the kinetics of enzymes involved in acyl-ACP elongation and hydrolysis. For instance, in *Cuphea palustris*, two MCFA-specific FatB isoforms with distinct acyl length preferences were expressed at similar levels in the developing embryo but displayed contrasted kinetics that concurred with oil FA composition (Dehesh et al., 1996). Taking advantage of recent transcriptomic technologies, this work investigates the contribution of a third key mode of regulation, i.e. the transcriptional control of genes involved in the competing branches of FA synthesis and release.

We identified three *FatB* paralogs and one *FatA* gene in the transcriptomes of the developing embryo, endosperm, and mesocarp of oil palm. Duplication and neofunctionalization of *FatB* genes is a common feature among plants that store MCFA (Jones et al., 1995; Voelker and Kinney, 2001). Three *FatB* genes were also identified in coconut, a close relative of oil palm (Jing et al., 2011). Each of the three oil palm FatB isoforms closely grouped with one of the three coconut FatB enzymes in our phylogenetic analysis, suggesting that gene triplication preceded the separation of the two species. Both our transient expression experiments in *N. benthamiana* leaves and transcriptomic data suggest that, among the three *FatB* paralogs identified, *EgFatB3* is the only paralog that encodes an MCFA-specific thioesterase in oil palm. Among the three coconut FatB isoforms, CnFatB3 shows the highest similarity with EgFatB3 and was the only isoform leading to 12:0 accumulation in *Escherichia coli* (Jing et al., 2011). In comparison with the two other *EgFatB* genes and *EgFatA*, the level of transcription of *EgFatB3* in the endosperm was extremely high and displayed the highest transcript amounts among all lipid-related genes during the stages of oil deposition. These important findings suggest that, in oil palm, to compete efficiently with acyl chain elongation, the premature cleavage of acyl-ACP requires the considerable up-regulation of the MCFA-specific *FatB* gene. Transcriptional patterns of *FatB* paralogs in the embryo confirmed this hypothesis. While the proportion of MCFA in embryo storage lipids was rather low (7%), the transcription level of *EgFatB3* was at least 2-fold higher than that of other *FatB* genes. To our knowledge, there is no transcriptomic data available in the literature that enables an investigation to whether this molecular mechanism occurs in other MCFA-producing species. Because the premature cleavage of acyl-ACP is competing with elongation, it is worth noting that KAS transcript amounts were similar in the endosperm and the mesocarp (Supplemental Table S1). Moreover, in contrast with *Cuphea* species that possess an additional MCFA-specific condensing enzyme (Dehesh et al., 1998; Slabaugh et al., 1998), we did not find an additional KAS isoform in the endosperm transcriptome. Considering the importance of the role played by KAS IV in *Cuphea* species, this suggests that different strategies might have evolved to enrich the acyl pool with MCFA. It seems that in oil palm it mostly relies on the dramatic up-regulation of a single FatB gene.

Another unexpected result was the absence of *FatA* transcripts in the embryo transcriptome though unsaturated FA represented about two-thirds of total FA. This suggests that either EgFatB1 or EgFatB2 displays high activity toward 18:1-ACP. Arabidopsis FatB displayed the highest activity toward 16:0-ACP but also displayed significant activity with 18:1-ACP (about 75% of that obtained with 16:0-ACP; Salas and Ohlrogge, 2002). Substrate specificity of only one oil palm FatB enzyme was characterized until now (Othman et al., 2000). Its sequence corresponded to the paralog *EgFatB2* from this work and the recombinant enzyme obtained from this clone displayed a marked preference for 16:0 over 12:0 and 18:1. This observation is in agreement with the high increase in the 16:0 level of TAG accumulated in leaves of *N. benthamiana* agroinfiltrated with *EgFatB2*, but does not provide an explanation for the high level of C18 FA in the embryo. The characterization of EgFatB1 substrate specificity could therefore help in understanding the FA profile of this tissue.

Tissue Transcriptional Specialization of WRI1 Paralogs in Oil Palm

Despite considerable progress in the understanding of the metabolic pathways involved in storage lipid biosynthesis and in the identification of the genes coding for the enzymes involved, our knowledge of the factors controlling oil accumulation in plant tissues remains incomplete (Baud and Lepiniec, 2010). Top-down control analysis experiments using oil palm callus cultures suggested that control is mostly exerted by FA synthesis in this species (Ramli et al., 2009), while TAG assembly primarily regulates oil accumulation in other species such as rape (Tang et al., 2012). Our previous finding that a WRI1-like transcription factor was massively accumulated in the mesocarp of oil palm at the onset of oil accumulation, concomitantly with the dramatic up-regulation of almost all FA biosynthetic genes, corroborated top-down control analysis experiments (Tranbarger et al., 2011). This result also showed that transcriptional activation of the FA biosynthetic machinery by WRI1 is not restricted to embryos and, together with the identification of two functional *WRI1* coorthologs in maize (Pouvreau et al., 2011), that FA synthesis regulation by WRI1 transcription factors occurred in plants before the separation of monocots and dicots. In this work, we provide

evidence for the existence of three *WRI1* copies with contrasting tissue transcriptional patterns. This important finding raises two distinct issues that have to be considered separately: the number of *WRI* copies and their orthologous/paralogous status, and tissue transcriptional specialization. Arabidopsis possesses four members of the WRINKLED clade, three of which (WRI1, WRI3, and WRI4) are transcriptional activators of the FA biosynthetic pathway (Baud et al., 2007; To et al., 2012). An in-depth phylogenetic analysis of maize sequences homologous to *AtWRI1* supports the existence of two *WRI1* copies in this species, and microsynteny analysis of the corresponding regions suggests they arose from a duplication event that occurred in the Poaceae ancestral genome (Pouvreau et al., 2011). Our phylogenetic analysis of oil palm *WRI1* sequences, together with those of Arabidopsis, rape, rice, and maize, perfectly reflects the early separation between the palm lineage (the order Arecales) and that of Poaceae (Al-Dous et al., 2011). It is difficult to ascertain the events that caused the triplication of *WRI1* in oil palm, but the high level of similarity among the three *EgWRI1* sequences and the absence of recent whole-genome duplication events in the order Arecales in comparison with other monocots make the case for small-scale duplications. For these reasons we use the term "paralogs" to describe *WRI1* gene copies in oil palm. Nevertheless, the evolution of this important plant gene family clearly requires further investigation.

In a very recent study, To et al. (2012) uncovered functional specialization of WRI transcription factors in Arabidopsis. In this species, WRI1, WRI3, and WRI4 are essential to floral organ formation but only WRI1 triggers FA synthesis in seeds. Our transcriptomic data revealed high tissue transcriptional specialization of *WRI1* paralogs in oil palm. *EgWRI1-2* and *EgWRI1-3* were exclusively transcribed in the endosperm, whereas *EgWRI1-1* was specific to the mesocarp. This divergence between tissues is much more pronounced than in the two maize *WRI1* genes whose transcriptional patterns also differed between the embryo and the endosperm, but to a much lesser extent given that both copies were significantly transcribed in both tissues (Pouvreau et al., 2011). None of the three oil palm *WRI1* paralogs were found in the transcriptome of developing inflorescences (James Tregear, personal communication) and leaf tissues (Bourgis et al., 2011).

The ability of *EgWRI1-1* and *EgWRI1-2* to trigger FA synthesis and subsequent oil accumulation was validated using transient expression in *N. benthamiana* leaves. It has previously been demonstrated that *ZmWRI1a* and *ZmWRI1b* complement Arabidopsis *wri1* mutants (Pouvreau et al., 2011), and this result confirms the high level of conservation among angiosperms of the *WRI1* DNA-binding domain and of the AW box sequence in the promoter of FA synthesis genes, which is considered the binding site for WRI1 (Maeo et al., 2009). We previously found AW box elements in the proximal region of six genes involved in FA synthesis in oil palm (Tranbarger et al., 2011). The transcriptomic sequences obtained in this work enabled the identification of 10 additional genes whose putative promoter sequences contain canonical AW box elements (Supplemental Table S2). However, *N. benthamiana* leaf TAG content was lower with *EgWRI1-2* than with *EgWRI1-1*, suggesting that amino acid sequence variations between the two *WRI1* paralogs (89% identity; Supplemental Data Set S5) may cause differential ability to activate *N. benthamiana* FA synthesis gene transcription.

We identified a positive relationship between the amounts of *WRI1* transcripts in oil palm tissues and the mean transcription level of FA synthesis genes, which in turn was correlated with the amount of oil stored. The existence of such a relationship implies that activation of FA synthesis by *WRI1* directs carbon toward oil metabolism in a quantitative manner. In maize embryos overexpressing *ZmWRI1*, the increase in oil content is at the expense of starch accumulation (Shen et al., 2010). Embryos of Arabidopsis *wri1* mutants transiently store increased amounts of starch, most likely because excess carbon is channeled to starch biosynthesis instead of TAG (Focks and Benning, 1998). In the oil palm endosperm, the lipid pathway is competing with cell wall storage polysaccharide (36% DM) and storage protein synthesis (Alang et al., 1988). One may therefore wonder whether relative proportions of these three main classes of storage compounds would be remodeled in favor of oil if the transcription level of *EgWRI1-2* in the developing endosperm would be as high as that of *EgWRI1-1* in the mesocarp. Because transformation techniques are not routinely available in oil palm to test this hypothesis, an alternative approach currently developed in our laboratory investigates the relationship between *WRI1* transcription level and oil accumulation within a large set of Arecaceae species that display a considerable variability for endosperm and mesocarp lipid content.

The analysis of the oil palm embryo transcriptome also evidenced that *WRI1* transcription is not a prerequisite for oil synthesis. This tissue accumulated up to 27% oil, whereas none of the three *WRI1* paralogs was detected. This is consistent with the observation that oil accumulation in Arabidopsis *wri1* mutant lines is severely impaired but not completely shut down (2–4 times lower; e.g. Focks and Benning, 1998; Baud et al., 2007; Pouvreau et al., 2011). This is also in agreement with the very low *WRI1* transcript abundance in the developing embryo of *Tropaeolum majus* and endosperm of *Euonymus alatus*, which accumulate 10% and 50% oil, respectively (Troncoso-Ponce et al., 2011). It may be speculated that transcription factors of other families control FA synthesis in these tissues. Alternatively, one can hypothesize that the upregulation of *DGAT* observed in the oil palm embryo is sufficient to capture a significant proportion of newly synthesized FA from basal metabolism into TAG and storage organelles. For instance, transient expression of *AtDGAT1* is sufficient to induce oil accumulation in *N. benthamiana* leaves (Vanhercke et al., 2013). However,

while an abrupt increase in oil content occurred in the endosperm and the mesocarp of oil palm at the onset of *WRI1* transcription, the embryo displayed a continuous oil accumulation throughout its development at a low rate. As previously observed with *EgWRI1-1* in the mesocarp (Tranbarger et al., 2011), transcripts of *EgWRI1-2* accumulated massively in the endosperm during oil deposition, and almost all genes involved in FA synthesis displayed the same transcriptional pattern as *EgWRI1-2* in this tissue. By contrast, genes involved in FA synthesis displayed a very weak temporal coordination in the embryo. Collectively these results thus suggest that a coordinated activation of the plastidial FA biosynthetic machinery within a precise period of development is the key role played by WRI1.

Between-Tissue Differences in the Conversion of Suc to Pyruvate Reflects Adaptation to Physiological Context Rather Than Variation for Oil Synthesis

Remarkably, the carbon assimilatory pathway identified for the oil palm mesocarp in this work resembles that observed in green photoheterotrophic seeds of rape and soybean (*Glycine max*), in which isozymes for PFK, Fru biphosphate aldolase, and GAPDH were almost equally abundant in the cytosol and the plastid (Hajduch et al., 2006; Agrawal et al., 2008). Conversely, the glycolytic route inferred from our transcriptome analysis in the two chlorophyll-less oil palm seed tissues (endosperm and embryo) is very similar to that reported for the nongreen heterotrophic seed of castor bean, in which nearly all glycolytic enzymes were cytosolic and the five lower glycolytic steps (from triose-P isomerase to ENO) predominate in terms of enzyme abundance in comparison with upstream steps (Houston et al., 2009). Hence, differences observed between green photoheterotrophic (e.g. rape, Arabidopsis) and heterotrophic seeds (e.g. castor [*Ricinus communis*]), at both proteomic and transcriptomic levels (Houston et al., 2009; Troncoso-Ponce et al., 2011) are basically the same as those observed here within a single species between a photoheterotrophic tissue (mesocarp) and heterotrophic ones (embryo and endosperm).

Due to the low permeability of maternal tissues for gases and their low surface area-to-volume ratio, seeds are described as microaerophilic environments, with subsequent lower ATP/ADP ratios (Borisjuk and Rolletschek, 2009). This phenomenon is exacerbated in heterotrophic seeds in which there is no photosynthetic oxygen release. In this respect, the chlorophyll-less endosperm and embryo of oil palm display features of adaptation to low oxygen conditions encountered in maturing seeds, such as transcriptional activation of PPi-dependent PFP instead of ATP-dependent PFK and of the PPi-consuming Suc synthase pathway (Baud and Graham, 2006; Baud and Lepiniec, 2010). In photoheterotrophic Arabidopsis seeds, the homeostasis of PPi is partly controlled through the catabolic activity of a cytosolic inorganic PPiase, the perturbation of which impacts oil synthesis (Meyer et al., 2012). In oil palm seed tissues, PPiase was not detected in the embryo and was faintly expressed in the endosperm compared with the mesocarp. The expression pattern of PFP in the three tissues was inversely correlated to that of PPiase, suggesting that PFP replaces PPiase in hypoxic seed tissues and plays a similar functional role in PPi/inorganic phosphate homeostasis. It is thus tempting to hypothesize that the absence of a plastidial PPi-dependent PFP in the genome of higher plants limits the contribution of the plastidial pathway under hypoxic conditions. Differences in the contribution of the two parallel glycolytic routes between photosynthetically active (oil palm mesocarp, rape, and Arabidopsis seeds) and heterotrophic (oil palm and castor seeds) would thus rather reflect adaptation to local physiological context than evolutionary divergences or quantitative variations for the amount of oil deposited.

Though the plastidial glycolytic pathway seems activated in the oil palm mesocarp, genes encoding enzymes that catalyze the reactions that convert 1.3PGA into PEP (PGK, PGLYM, and ENO) were transcribed at a very low level in this compartment. In embryos of rape and soybean, plastidial isoforms of PGLYM and ENO were also not detected (Hajduch et al., 2006; Agrawal et al., 2008). It was thus hypothesized that, in these species, the pool of triose-P produced by plastidial glycolysis is transported to the cytosol by TPT and converted to PEP, which is then transported back into the plastid by PEP translocator before conversion to pyruvate. Metabolic flux analysis in developing rape embryos confirmed the occurrence of rapid exchanges of triose-P between the two compartments (Schwender et al., 2003). Characterization of Arabidopsis mutants for plastidial PGLYM and ENO also supports the hypothesis for a rather limited role of these enzymes in Arabidopsis green seeds and highlights the importance of TPT (Andriotis et al., 2010). In conclusion, the transcriptional status of plastidial forms of PGK, PGLYM, and ENO in the oil palm mesocarp may represent another functional feature shared with green photoheterotrophic seeds.

TAG Assembly in the Endosperm of Cocoseae Palm Species

Neither CPT nor PDCT transcripts were detected in the developing oil palm endosperm, suggesting that PC-DAG interconversion is shut down in this tissue during oil biosynthesis. Using ^{14}C-labeled glycerol, acyl-CoA preference was compared in microsomal preparations from seeds of rape, maize, and *Butia capitata* (a palm species phylogenetically close to oil palm, tribe *Cocoseae*; Sun et al., 1988). This study not only revealed that 12:0-CoA was incorporated in 1,2-diacylglycerol-3-P (PA) and TAG with *B. capitata* microsomes only, but also that no labeled PC was detected in this palm species, while substantial amounts of labeled PC were produced with maize and rape microsomes. This result

corroborates remarkably our finding that genes encoding enzymes that enable PC-DAG interconversion are not transcribed during oil biosynthesis in the endosperm. This is very likely a mechanism that prevents incorporation of MCFA in membranes. MCFAs are known to perturb the structural integrity of membrane bilayers (Millar et al., 2000).

Another mechanism allowing the partitioning of MCFA and long-chain FA (C18) in neutral and membrane lipids, respectively, has been identified in *Cuphea* species that store MCFA. It was shown in these species that LPAAT preferentially uses a C18-FA when the FA esterified at the *sn*-1 position is a C18-FA, whereas if a MCFA is at the at the *sn*-1 position, it exclusively transfers a MCFA at the *sn*-2 position, thus preventing the formation of mixed MCFA-C18 PA (Bafor et al., 1990). DAG esterified with two MCFA are then efficiently directed to TAG production because of the preference and selectivity of *Cuphea* spp. DGAT for this category of DAG molecular species (Wiberg et al., 1994; Vogel and Browse, 1996). Although substrate preference of oil palm LPAAT-B has not been investigated, characterization of LPAAT from close relatives of oil palm suggests that the mechanism identified in *Cuphea* species to exclude MCFA from membranes does not exist in palm species. The endosperm-specific LPAAT-B enzyme from coconut (tribe Cocoseae), whose sequence is highly similar to that of EgLPAAT-B, efficiently uses both 12:0-CoA and 18:1-CoA when the lyso-PA was esterified with 12:0 at the *sn*-1 position (Davies et al., 1995). Microsomal LPAAT of *Syagrus cocoides* (tribe Cocoseae) was also shown to produce as much mixed MCFA-C18 PA as unmixed PA (Laurent and Huang, 1992). Since plants accumulating unusual FA have evolved independently, it is accepted that the mechanisms used for their exclusion from membrane bilayers differ between species (Millar et al., 2000). Our results, together with those reported in other palm species, suggest that switching off CPT during oil biosynthesis might represent the main mechanism for MCFA exclusion in the endosperm of Cocoseae species. In this respect, it is worth noting that CPT does not show selectivity for C18-DAG in plants accumulating unusual FA. Vogel and Browse (1996) demonstrated that CPT in seeds of *Cuphea lanceolata*, castor bean (which accumulates hydroxy-FA), safflower (*Carthamus tinctorius*), and rape show very little specificity across a wide range of DAG substrates.

Another point of entry of MCFA in membrane lipids, which received little attention until now in the literature dedicated to plants that store MCFA, is the exchange of FA between the acyl-CoA pool and the PC pool, referred to as the acyl editing mechanism (Bates et al., 2009). The importance of this process during oil biosynthesis in various oilseeds has emerged recently (Bates and Browse, 2012; Chapman and Ohlrogge, 2012). LPCAT enzymes play a central role in acyl editing (Wang et al., 2012). They may achieve acyl exchange between the two pools by themselves or incorporate newly synthesized FA into the PC pool using lyso-PC resulting from either PDAT or PLA2 activity. We identified two tissue-specific LPCAT isoforms in the transcriptome of oil palm tissues, of which EgLPCAT-2 is exclusive to the endosperm. Because of the predominance of MCFA in the endosperm acyl-CoA pool, the recruitment of a specific isoform in this tissue could constitute another mechanism to prevent the incorporation of MCFA into membranes. This hypothesis implies that this isoform would display a marked preference for C18 FA in comparison with EgLPACT-1.

CONCLUSION

The comparative analysis of the three TAG accumulating tissues of oil palm showed that transcriptional regulation plays a key role in the considerable differences in oil content and FA composition that exist between these tissues. Fine-tuned modulation of *EgFAD2* and *EgFAD3* transcription appeared to control tissue variation for PUFA levels. MCFA accumulation in the endosperm of oil palm, and most likely of many species of the tribe Cocoseae, seems to rely on tissue-specific up-regulation of neofunctionalized paralogs such as *EgFatB3* and transcriptional shutdown of PC-DAG interconversion. We also evidenced tissue transcriptional specialization of *WRI1* paralogs in oil palm, which brings to mind organ-specific regulation of FA synthesis by distinct members of the WRI clade in Arabidopsis (To et al., 2012). Conversely, this work revealed no tissue transcriptional specialization for the plastidial steps involved in de novo FA synthesis. This important finding corroborates transcriptomic observations made in two studies, carried out at the between-species and between-tissue levels, respectively. Oil seeds of four unrelated species preferentially use the same isoform for most FA biosynthetic steps (Troncoso-Ponce et al., 2011). The perisperm and endosperm of the coffee seed also employ the same gene copy for these reactions (Joët et al., 2009). This strengthens the hypothesis for the conservation of a common set of isoforms for storage lipid synthesis throughout plant evolution (Troncoso-Ponce et al., 2011). However, the choice of the gene copy recruited at each step of de novo FA synthesis seems strictly independent of *WRI1* paralog transcriptional status. This reinforces the view that the main role of WRI1 transcription factors is to trigger high rates of acyl chain production when and where needed (To et al., 2012). Nonetheless, the identification of the regulatory cascade that controls *WRI1* expression in oil palm fruit and seed tissues remains an unsolved critical issue. The knowledge gained in Arabidopsis (Baud et al., 2007; Mu et al., 2008; Yamamoto et al., 2010) and Poaceae (Shen et al., 2010) on the activation of *WRI1* by the master regulators of the seed maturation process is apparently not applicable to Arecaceae. Finally, considering the crucial role played by acyl-ACP thioesterases, the identification of factors that control *FatA* and *FatB* transcription is one of most exciting challenges for future research in oil palm.

MATERIALS AND METHODS

Plant Material

Oil palm (*Elaeis guineensis*) fruits were harvested at the Centre de Recherches Agricoles Plantes Pérennes station (Pobé, Bénin) from a *dura* parent of Deli Dabou origin, within the same self-progeny of a single tree. For each stage of development studied, three independent bunches were harvested on three distinct individuals of the same genotype. Fifteen spikelets were then collected in the center of each bunch and five spikelets were randomly sampled from them. From all undamaged fruits withdrawn from each of the five spikelets, three fruits were then randomly sampled. Then, for each stage × bunch × spikelet combination retained, mesocarp, endosperm, and embryo of each fruit were separated, weighed, and flash frozen in liquid nitrogen.

Histology and Lipid Analysis

To visualize lipids in the endosperm and the embryo, tissue samples were sectioned (100 μm) using vibratom, washed with PBS 1X, then stained with Nile red and analyzed by confocal microscopy (Zeiss LM510), with a laser excitation at 458 nm and a HFT filter 548/514 using the 40×/1.2 numerical aperture. Total lipids were extracted from samples of freeze-dried powder using a modified Folch method as described previously (Laffargue et al., 2007). Fatty acid methyl esters (FAME) were prepared according to the ISO-5509 standard, and gas chromatography analyses of FAME were performed as previously described (Laffargue et al., 2007). For each tissue and each stage of development, lipid analyses were performed in triplicate (from three different extractions) using a completely random experimental design.

Pyrosequencing, Contig Assembly, and Annotation

Total RNA from endosperm (70, 85, 100, 120, and 160 DAP) was extracted as described in Argout et al. (2008). Total RNA from embryos (85, 90, 100, 120, and 160 DAP) was extracted using the lipid RNeasy Plant Kit (Qiagen). Mesocarp transcriptomic data used in this study were obtained in a previous study using the same fruit samples (Tranbarger et al., 2011). For each seed tissue, complementary DNA related to all stages of development were tagged independently (Titanium kit, Roche Diagnostics) then mixed together for 454 pyrosequencing carried out by GATC Biotech AG (Germany) using GS FLX Titanium (Roche). De novo assembly of contigs was performed as described in Tranbarger et al. (2011). Endosperm and embryo contigs were assembled separately. Identification of contigs related to sugar and lipid metabolism was performed using Arabidopsis (*Arabidopsis thaliana*) sequences from The Arabidopsis Information Resource database, tblastx, and an E-value cut off of E^{-25} (E^{-20} for oleosins and caleosins). Annotation of resulting contigs was refined using blastx and the National Center for Biotechnology Information nonredundant protein sequence database. Information available at http://aralip.plantbiology.msu.edu/ was also used to refine contig annotation. For between-tissue comparison, two contigs from distinct tissues were considered to correspond to the same gene copy when they displayed greater than 99% nucleotide identity. Search for AW box in the proximal region of transcripts was performed using MatInspector of the Genomatix software suite (http://www.genomatix.de/).

Statistical Analysis of Read Abundance Profiles and Phylogenetic Analysis

A contig was considered differentially expressed during development when at least stage transition exhibited a highly significant difference in read abundance at $P = 0.01$. Difference in read abundance between two stages of development was tested using AC statistics (Audic and Claverie, 1997). P values obtained by the AC test were then transformed using the Bonferroni correction to control FDRs. HCA was used to group contigs according to their transcription profile, using the tool developed by Eisen et al. (1998). Phylogenetic analyses were performed on the Phylogeny.fr platform (http://www.phylogeny.fr; Dereeper et al., 2008) as described in Tranbarger et al. (2011).

Plasmid Constructs

The complete open reading frame of *EgFATB1*, *EgFATB2*, *EgFATB3*, *EgWRI1-1*, and *EgWRI1-2* was amplified by PCR using the following primer pairs: CACCATGGTTGCTTCGATTGCCG/ TCAAGCACTTCCAGCTGAA, CACCATGGTTGCTTCAATTGCCG/TCATGCACTACCACCTGGAG, CACCATGGTC GCCTCCGTTGCTG/TCATTTAGTCTCAGTTGGGAG, CACCATGACTCTCATGAAGAACT/CTAGGCACCTTTGCT TGCACTGA, and CACCATGAAGAAATCTCCTCCCT/CTAGGCACCCTGGCTTGTA, respectively. PCR fragments were cloned into the Gateway-pENTR/D-Topo vector (Invitrogen) then placed adjacent to a dual 35S Cauliflower Mosaic Virus promoter in the destination vector pMDC32 (Curtis and Grossniklaus, 2003) through LR clonase reactions (Invitrogen). *p19* (Voinnet et al., 2003) and *GFP* (Wood et al., 2009) constructs were kindly provided by Dr. Craig Wood (Commonwealth Scientific and Industrial Research Organization, Australia).

Agroinfiltration of *Nicotiana benthamiana*

Agrobacterium tumefaciens GV3101:pMP90 (Koncz and Schell, 1986) harboring the individual vectors were grown in lysogeny broth supplemented with appropriate antibiotics (50 μg mL^{-1} rifampicin and 50 μg mL^{-1} kanamycin or 50 μg mL^{-1} spectinomycin) at 28°C overnight. One hundred micromolars of acetosyringone was added to cultures and grown for an additional 3 h. Cultures were harvested by centrifugation at 2,800 rpm for 8 min at 18°C and gently resuspended in 0.5 volumes infiltration media (5 mM MES and 5 mM $MgCl_2$, pH 5.7). Optical densities at 600 nm were measured and each culture diluted in infiltration media to yield an optical density of 0.2 in the final infiltration solution. Coexpression was performed by mixing *GFP* and *p19* wit h the oil palm genes of interest. Prior infiltration 100 μM acetosyringone was added to the mixture of cells.

Agroinfiltration was performed as described in Wood et al. (2009) with minor modifications. Wild-type *N. benthamiana* plants were grown in a growth chamber at 26°C, 60% relative humidity, with a 12-h photoperiod (250 μmol m^{-2} s^{-1}) for 6 weeks. Infiltration was made on young developing leaves on freshly watered plants, using a 1-mL syringe without a needle on the underside of the leaf tissue, until an area of at least 7 cm^2 was infiltrated. Plants were returned to the growth cabinet for an additional 5 d. The infiltrated leaf areas were cut out and fresh weight measured. When the infiltrated area was not visible with the naked eye, a hand-held fluorescent protein flashlight (DFP-1, NightSea) was used to track the GFP expression. The harvested leaf tissues were freeze dried (Scanvac Cool safe, Scanlaf) for 3 d before dry weights were measured and extraction of lipids were made.

Lipids were extracted from harvested leaf tissues by homogenization in 3.75 mL methanol/chloroform (2:1, v/v) following the method described by Bligh and Dyer (1959). Extracted lipids from 100 mg fresh weight leaf tissue were separated using thin layer chromatography (Silica 60 plates, Merck) and heptane/diethylether/acetic acid (70/30/1, v/v/v). TAG were visualized by spraying the thin layer chromatography plate with 0.05% primuline (in acetone: water, 8:2, v/v) and imaged under UV light. The spot of TAG was collected followed by methylation to produce FAME. Gas chromatography analysis (GC-17A, Shimadzu) was performed as previously described by Doan et al. (2012). Hydrogen was used as a carrier gas at a column flow rate of 2.64 mL min^{-1}. The injection and detection temperatures were 230°C and 270°C, respectively. An initial temperature of 100°C was held for 2 min followed by an increase in temperature to 230°C at a rate of 11°C per minute and held for 10 min. FA profiles and quantities of TAG were calculated using reference mixture (Me 63, LGC standards) and internal standard heptadecalon (50–100 nmol).

Supplemental Data

The following materials are available in the online version of this article.

Supplemental Figure S1. Hierarchical Cluster Analysis (HCA) of differentially expressed contigs in the developing endosperm according to Audic-Claverie and FDR statistics.

Supplemental Figure S2. Changes in transcript abundance during the development of the oil palm endosperm (DAP) of the 14 differentially expressed contigs involved in FA synthesis that co-clustered in Cluster Aa and two copies of the transcription factor WRI1

Supplemental Figure S3. Phylogenetic analysis of the four oil palm acyl-ACP thioesterases identified in the transcriptomes of the developing embryo, endosperm, and mesocarp, using multiple alignment of the enzymatic FAT domains and the neighbor joining method.

Supplemental Figure S4. Phylogenetic analysis of the two oil palm lysophosphatidic acid acyltransferases identified in the transcriptomes of the

developing embryo, endosperm, and mesocarp, using multiple alignment of full-length protein sequences and the neighbor joining method.

Supplemental Figure S5. Phylogenetic analysis of the three oil palm acyl-CoA:diacylglycerol acyltransferase identified in the transcriptomes of the developing embryo, endosperm, and mesocarp, using multiple alignment of full-length protein sequences and the neighbor joining method.

Supplemental Table S1. Temporal profile of lipid- and sugar-related genes in the developing embryo, endosperm, and mesocarp.

Supplemental Table S2. Identification of AW box elements in the proximal upstream region of oil palm lipid-related genes using the Genomatix software suite (http://www.genomatix.de).

Supplemental Data Set S1. Embryo transcriptome: FASTA sequences of contigs represented by at least 20 reads per million reads over all stages of development.

Supplemental Data Set S2. Endosperm transcriptome: FASTA sequences of contigs represented by at least 20 reads per million reads over all stages of development.

Supplemental Data Set S3. Mesocarp transcriptome: FASTA sequences of contigs represented by at least 20 reads per million reads over all stages of development.

Supplemental Data Set S4. FASTA sequences of oil palm lipid-related genes.

Supplemental Data Set S5. CLUSTAL 2.1 multiple sequence alignment of double AP2 domains of the three EgWRI1 isoforms.

ACKNOWLEDGMENTS

We would also like to especially thank all the personnel at Institut National des Recherches Agricoles du Bénin, Centre de Recherches Agricoles Plantes Pérennes, Pobé, Benin for their technical and logistical support during the collection of the material used in this study and Myriam Collin for her assistance with the histological analysis.

Received April 26, 2013; accepted May 29, 2013; published June 5, 2013.

LITERATURE CITED

Agrawal GK, Hajduch M, Graham K, Thelen JJ (2008) In-depth investigation of the soybean seed-filling proteome and comparison with a parallel study of rapeseed. Plant Physiol **148:** 504–518

Alang ZC, Moir GFJ, Jones LH (1988) Composition, degradation and utilization of endosperm during germination in the oil palm (*Elaeis guineensis* Jacq.). Ann Bot (Lond) **61:** 261–268

Al-Dous EK, George B, Al-Mahmoud ME, Al-Jaber MY, Wang H, Salameh YM, Al-Azwani EK, Chaluvadi S, Pontaroli AC, DeBarry J, et al (2011) *De novo* genome sequencing and comparative genomics of date palm (*Phoenix dactylifera*). Nat Biotechnol **29:** 521–527

Allen DK, Young JD (2013) Carbon and nitrogen provisions alter the metabolic flux in developing soybean embryos. Plant Physiol **161:** 1458–1475

Alonso AP, Goffman FD, Ohlrogge JB, Shachar-Hill Y (2007) Carbon conversion efficiency and central metabolic fluxes in developing sunflower (*Helianthus annuus* L.) embryos. Plant J **52:** 296–308

Andriotis VM, Kruger NJ, Pike MJ, Smith AM (2010) Plastidial glycolysis in developing Arabidopsis embryos. New Phytol **185:** 649–662

Argout X, Fouet O, Wincker P, Gramacho K, Legavre T, Sabau X, Risterucci AM, Da Silva C, Cascardo J, Allegre M, et al (2008) Towards the understanding of the cocoa transcriptome: Production and analysis of an exhaustive dataset of ESTs of *Theobroma cacao* L. generated from various tissues and under various conditions. BMC Genomics **9:** 512

Audic S, Claverie JM (1997) The significance of digital gene expression profiles. Genome Res **7:** 986–995

Bafor M, Jonsson L, Stobart AK, Stymne S (1990) Regulation of triacylglycerol biosynthesis in embryos and microsomal preparations from the developing seeds of *Cuphea lanceolata*. Biochem J **272:** 31–38

Bafor M, Stymne S (1992) Substrate specificities of glycerol acylating enzymes from developing embryos of two *Cuphea* species. Phytochemistry **31:** 2973–2976

Bates PD, Durrett TP, Ohlrogge JB, Pollard M (2009) Analysis of acyl fluxes through multiple pathways of triacylglycerol synthesis in developing soybean embryos. Plant Physiol **150:** 55–72

Bates PD, Browse J (2012) The significance of different diacylgycerol synthesis pathways on plant oil composition and bioengineering. Front Plant Sci **3:** 147

Baud S, Graham IA (2006) A spatiotemporal analysis of enzymatic activities associated with carbon metabolism in wild-type and mutant embryos of Arabidopsis using *in situ* histochemistry. Plant J **46:** 155–169

Baud S, Mendoza MS, To A, Harscoët E, Lepiniec L, Dubreucq B (2007) WRINKLED1 specifies the regulatory action of LEAFY COTYLEDON2 towards fatty acid metabolism during seed maturation in Arabidopsis. Plant J **50:** 825–838

Baud S, Lepiniec L (2010) Physiological and developmental regulation of seed oil production. Prog Lipid Res **49:** 235–249

Bligh EG, Dyer WJ (1959) A rapid method of total lipid extraction and purification. Can J Biochem Physiol **37:** 911–917

Borisjuk L, Rolletschek H (2009) The oxygen status of the developing seed. New Phytol **182:** 17–30

Bourgis F, Kilaru A, Cao X, Ngando-Ebongue GF, Drira N, Ohlrogge JB, Arondel V (2011) Comparative transcriptome and metabolite analysis of oil palm and date palm mesocarp that differ dramatically in carbon partitioning. Proc Natl Acad Sci USA **108:** 12527–12532

Cernac A, Benning C (2004) WRINKLED1 encodes an AP2/EREB domain protein involved in the control of storage compound biosynthesis in Arabidopsis. Plant J **40:** 575–585

Chapman KD, Ohlrogge JB (2012) Compartmentation of triacylglycerol accumulation in plants. J Biol Chem **287:** 2288–2294

Curtis MD, Grossniklaus U (2003) A gateway cloning vector set for high-throughput functional analysis of genes in planta. Plant Physiol **133:** 462–469

Davies HM, Hawkins DJ, Nelsen JS (1995) Lysophosphatidic acid acyltransferase from immature coconut endosperm having medium chain length substrate specificity. Phytochemistry **39:** 989–996

Dehesh K, Edwards P, Hayes T, Cranmer AM, Fillatti J (1996) Two novel thioesterases are key determinants of the bimodal distribution of acyl chain length of *Cuphea palustris* seed oil. Plant Physiol **110:** 203–210

Dehesh K, Edwards P, Fillatti J, Slabaugh M, Byrne J (1998) KAS IV: a 3-ketoacyl-ACP synthase from *Cuphea sp*. is a medium chain specific condensing enzyme. Plant J **15:** 383–390

Dehesh K (2001) How can we genetically engineer oilseed crops to produce high levels of medium-chain fatty acids? Eur J Lipid Sci Technol **103:** 688–697

Dereeper A, Guignon V, Blanc G, Audic S, Buffet S, Chevenet F, Dufayard JF, Guindon S, Lefort V, Lescot M, et al (2008) Phylogeny.fr: robust phylogenetic analysis for the non-specialist. Nucleic Acids Res **36:** W465–W469

Doan TTP, Domergue F, Fournier AE, Vishwanath SJ, Rowland O, Moreau P, Wood CC, Carlsson AS, Hamberg M, Hofvander P (2012) Biochemical characterization of a chloroplast localized fatty acid reductase from *Arabidopsis thaliana*. BBA-Mol Cell Biol L **1821:** 1244–1255

Dörmann P, Spener F, Ohlrogge JB (1993) Characterization of two acyl-acyl carrier protein thioesterases from developing *Cuphea* seeds specific for medium-chain- and oleoyl-acyl carrier protein. Planta **189:** 425–432

Dörmann P, Voelker TA, Ohlrogge JB (2000) Accumulation of palmitate in Arabidopsis mediated by the acyl-acyl carrier protein thioesterase FATB1. Plant Physiol **123:** 637–644

Durrett TP, Benning C, Ohlrogge J (2008) Plant triacylglycerols as feedstocks for the production of biofuels. Plant J **54:** 593–607

Dyer JM, Stymne S, Green AG, Carlsson AS (2008) High-value oils from plants. Plant J **54:** 640–655

Eisen MB, Spellman PT, Brown PO, Botstein D (1998) Cluster analysis and display of genome-wide expression patterns. Proc Natl Acad Sci USA **95:** 14863–14868

Focks N, Benning C (1998) *wrinkled1*: A novel, low-seed-oil mutant of Arabidopsis with a deficiency in the seed-specific regulation of carbohydrate metabolism. Plant Physiol **118:** 91–101

Frentzen M (1998) Acyltransferases from basic science to modified seed oils. Eur J Lipid Sci Technol **100:** 161–166

Gouk SW, Cheng SF, Ong ASH, Chuah CH (2012) Rapid and direct quantitative analysis of positional fatty acids in triacylglycerols using 13C NMR. Eur J Lipid Sci Technol **114:** 510–519

Hajduch M, Casteel JE, Hurrelmeyer KE, Song Z, Agrawal GK, Thelen JJ (2006) Proteomic analysis of seed filling in *Brassica napus*. Developmental characterization of metabolic isozymes using high-resolution two-dimensional gel electrophoresis. Plant Physiol **141:** 32–46

Houston NL, Hajduch M, Thelen JJ (2009) Quantitative proteomics of seed filling in castor: comparison with soybean and rapeseed reveals differences between photosynthetic and nonphotosynthetic seed metabolism. Plant Physiol **151:** 857–868

Jing F, Cantu DC, Tvaruzkova J, Chipman JP, Nikolau BJ, Yandeau-Nelson MD, Reilly PJ (2011) Phylogenetic and experimental characterization of an acyl-ACP thioesterase family reveals significant diversity in enzymatic specificity and activity. BMC Biochem **12:** 44

Joët T, Laffargue A, Salmona J, Doulbeau S, Descroix F, Bertrand B, de Kochko A, Dussert S (2009) Metabolic pathways in tropical dicotyledonous albuminous seeds: *Coffea arabica* as a case study. New Phytol **182:** 146–162

Jones A, Davies HM, Voelker TA (1995) Palmitoyl-acyl carrier protein (ACP) thioesterase and the evolutionary origin of plant acyl-ACP thioesterases. Plant Cell **7:** 359–371

Knutzon DS, Lardizabal KD, Nelsen JS, Bleibaum JL, Davies HM, Metz JG (1995) Cloning of a coconut endosperm cDNA encoding a 1-acyl-sn-glycerol-3-phosphate acyltransferase that accepts medium-chain-length substrates. Plant Physiol **109:** 999–1006

Koncz C, Schell J (1986) The promoter of TL-DNA gene 5 controls the tissue-specific expression of chimeric genes carried by a novel type of Agrobacterium binary vector. Mol Gen Genet **204:** 383–396

Laffargue A, de Kochko A, Dussert S (2007) Development of solid-phase extraction and methylation procedures to analyse free fatty acids in lipid-rich seeds. Plant Physiol Biochem **45:** 250–257

Laurent P, Huang AHC (1992) Organ- and development-specific acyl coenzyme a lysophosphatidate acyltransferases in palm and meadowfoam. Plant Physiol **99:** 1711–1715

Lersten NR, Czlapinski AR, Curtis JD, Freckmann R, Horner HT (2006) Oil bodies in leaf mesophyll cells of angiosperms: overview and a selected survey. Am J Bot **93:** 1731–1739

Li-Beisson Y, Shorrosh B, Beisson F, Andersson MX, Arondel V, Bates PD, Baud S, Bird D, Debono A, Durrett TP, et al (2013) Acyl-lipid metabolism. The Arabidopsis Book **11:** e0161, doi/10.1199/tab.0161

Liu J, Hua W, Zhan G, Wei F, Wang X, Liu G, Wang H (2010) Increasing seed mass and oil content in transgenic Arabidopsis by the overexpression of wri1-like gene from *Brassica napus*. Plant Physiol Biochem **48:** 9–15

Lu C, Xin Z, Ren Z, Miquel M, Browse J (2009) An enzyme regulating triacylglycerol composition is encoded by the ROD1 gene of Arabidopsis. Proc Natl Acad Sci USA **106:** 18837–18842

Maeo K, Tokuda T, Ayame A, Mitsui N, Kawai T, Tsukagoshi H, Ishiguro S, Nakamura K (2009) An AP2-type transcription factor, WRINKLED1, of Arabidopsis thaliana binds to the AW-box sequence conserved among proximal upstream regions of genes involved in fatty acid synthesis. Plant J **60:** 476–487

Meyer K, Stecca KL, Ewell-Hicks K, Allen SM, Everard JD (2012) Oil and protein accumulation in developing seeds is influenced by the expression of a cytosolic pyrophosphatase in Arabidopsis. Plant Physiol **159:** 1221–1234

Millar AA, Smith MA, Kunst L (2000) All fatty acids are not equal: discrimination in plant membrane lipids. Trends Plant Sci **5:** 95–101

Mu J, Tan H, Zheng Q, Fu F, Liang Y, Zhang J, Yang X, Wang T, Chong K, Wang XJ, et al (2008) *LEAFY COTYLEDON1* is a key regulator of fatty acid biosynthesis in Arabidopsis. Plant Physiol **148:** 1042–1054

Neuberger T, Sreenivasulu N, Rokitta M, Rolletschek H, Göbel C, Rutten T, Radchuk V, Feussner I, Wobus U, Jakob P, et al (2008) Quantitative imaging of oil storage in developing crop seeds. Plant Biotechnol J **6:** 31–45

Oo KC, Lee KB, Ong ASH (1986) Changes in fatty acid composition of the lipid classes in the developing oil palm mesocarp. Phytochemistry **25:** 405–407

Othman A, Lazarus C, Fraser T, Stobart K (2000) Cloning of a palmitoyl-acyl carrier protein thioesterase from oil palm. Biochem Soc Trans **28:** 619–622

Pirtle RM, Yoder DW, Huynh TT, Nampaisansuk M, Pirtle IL, Chapman KD (1999) Characterization of a palmitoyl-acyl carrier protein thioesterase (FatB1) in cotton. Plant Cell Physiol **40:** 155–163

Plaxton WC (1996) The organization and regulation of plant glycolysis. Annu Rev Plant Physiol Plant Mol Biol **47:** 185–214

Pollard MR, Anderson L, Fan C, Hawkins DJ, Davies HM (1991) A specific acyl-ACP thioesterase implicated in medium-chain fatty acid production in immature cotyledons of *Umbellularia californica.* Arch Biochem Biophys **284:** 306–312

Pouvreau B, Baud S, Vernoud V, Morin V, Py C, Gendrot G, Pichon JP, Rouster J, Paul W, Rogowsky PM (2011) Duplicate maize *Wrinkled1* transcription factors activate target genes involved in seed oil biosynthesis. Plant Physiol **156:** 674–686

Ramli US, Salas JJ, Quant PA, Harwood JL (2009) Use of metabolic control analysis to give quantitative information on control of lipid biosynthesis in the important oil crop, *Elaeis guineensis* (oilpalm). New Phytol **184:** 330–339

Ruuska SA, Girke T, Benning C, Ohlrogge JB (2002) Contrapuntal networks of gene expression during *Arabidopsis* seed filling. Plant Cell **14:** 1191–1206

Salas JJ, Ohlrogge JB (2002) Characterization of substrate specificity of plant FatA and FatB acyl-ACP thioesterases. Arch Biochem Biophys **403:** 25–34

Schwender J, Ohlrogge JB (2002) Probing in vivo metabolism by stable isotope labeling of storage lipids and proteins in developing *Brassica napus* embryos. Plant Physiol **130:** 347–361

Schwender J, Ohlrogge JB, Shachar-Hill Y (2003) A flux model of glycolysis and the oxidative pentosephosphate pathway in developing *Brassica napus* embryos. J Biol Chem **278:** 29442–29453

Schwender J, Goffman F, Ohlrogge JB, Shachar-Hill Y (2004) Rubisco without the Calvin cycle improves the carbon efficiency of developing green seeds. Nature **432:** 779–782

Schwender J, Shachar-Hill Y, Ohlrogge JB (2006) Mitochondrial metabolism in developing embryos of *Brassica napus.* J Biol Chem **281:** 34040–34047

Shen B, Allen WB, Zheng P, Li C, Glassman K, Ranch J, Nubel D, Tarczynski MC (2010) Expression of *ZmLEC1* and *ZmWRI1* increases seed oil production in maize. Plant Physiol **153:** 980–987

Slabaugh MB, Leonard JM, Knapp SJ (1998) Condensing enzymes from *Cuphea wrightii* associated with medium chain fatty acid biosynthesis. Plant J **13:** 611–620

Sun C, Cao YZ, Huang AHC (1988) Acyl coenzyme a preference of the glycerol phosphate pathway in the microsomes from the maturing seeds of palm, maize, and rapeseed. Plant Physiol **88:** 56–60

Tang M, Guschina IA, O'Hara P, Slabas AR, Quant PA, Fawcett T, Harwood JL (2012) Metabolic control analysis of developing oilseed rape (*Brassica napus* cv Westar) embryos shows that lipid assembly exerts significant control over oil accumulation. New Phytol **196:** 414–426

To A, Joubès J, Barthole G, Lécureuil A, Scagnelli A, Jasinski S, Lepiniec L, Baud S (2012) WRINKLED transcription factors orchestrate tissue-specific regulation of fatty acid biosynthesis in *Arabidopsis.* Plant Cell **24:** 5007–5023

Tranbarger TJ, Dussert S, Joët T, Argout X, Summo M, Champion A, Cros D, Omore A, Nouy B, Morcillo F (2011) Regulatory mechanisms underlying oil palm fruit mesocarp maturation, ripening, and functional specialization in lipid and carotenoid metabolism. Plant Physiol **156:** 564–584

Troncoso-Ponce MA, Kilaru A, Cao X, Durrett TP, Fan J, Jensen JK, Thrower NA, Pauly M, Wilkerson C, Ohlrogge JB (2011) Comparative deep transcriptional profiling of four developing oilseeds. Plant J **68:** 1014–1027

Vanhercke T, El Tahchy A, Shrestha P, Zhou XR, Singh SP, Petrie JR (2013) Synergistic effect of WRI1 and DGAT1 coexpression on triacylglycerol biosynthesis in plants. FEBS Lett **587:** 364–369

Voelker T, Kinney AJ (2001) Variations in the biosynthesis of seed-storage lipids. Annu Rev Plant Physiol Plant Mol Biol **52:** 335–361

Vogel G, Browse J (1996) Cholinephosphotransferase and diacylglycerol acyltransferase. Substrate specificities at a key branch point in seed lipid metabolism. Plant Physiol **110:** 923–931

Voinnet O, Rivas S, Mestre P, Baulcombe D (2003) An enhanced transient expression system in plants based on suppression of gene silencing by the p19 protein of tomato bushy stunt virus. Plant J **33:** 949–956

Wang L, Shen W, Kazachkov M, Chen G, Chen Q, Carlsson AS, Stymne S, Weselake RJ, Zou J (2012) Metabolic interactions between the Lands cycle and the Kennedy pathway of glycerolipid synthesis in *Arabidopsis* developing seeds. Plant Cell **24:** 4652–4669

Wiberg E, Tillberg E, Stymne S (1994) Substrates of diacylglycerol acyltransferase in microsomes from developing oil seeds. Phytochemistry **36:** 573–577

Wiberg E, Bafor M (1995) Medium-chain length fatty acid in lipids of developing oil palm kernel endosperm. Phytochemistry **39:** 1325–1327

Willett WC (2012) Dietary fats and coronary heart disease. J Intern Med **272:** 13–24

Wood CC, Petrie JR, Shrestha P, Mansour MP, Nichols PD, Green AG, Singh SP (2009) A leaf-based assay using interchangeable design principles to rapidly assemble multistep recombinant pathways. Plant Biotechnol J **7:** 914–924

Yamamoto A, Kagaya Y, Usui H, Hobo T, Takeda S, Hattori T (2010) Diverse roles and mechanisms of gene regulation by the Arabidopsis seed maturation master regulator FUS3 revealed by microarray analysis. Plant Cell Physiol **51:** 2031–2046

Ye R, Yao QH, Xu ZH, Xue HW (2004) Development of an efficient method for the isolation of factors involved in gene transcription during rice embryo development. Plant J **38:** 348–357